



# HIStory of LAND transformation by humans in South America (HISLAND-SA): annual and 1-km crop-specific gridded data (1950-2020)

Binyuan Xu<sup>1,2</sup>, Hanqin Tian<sup>1,3</sup>, Shufen Pan<sup>1,4</sup>, Xiaoyong Li<sup>1,5</sup>, Ran Meng<sup>6,13</sup>, Óscar Melo<sup>7</sup>,  
5 Anne McDonald<sup>8</sup>, María de los Ángeles Picone<sup>9</sup>, Xiao-Peng Song<sup>10</sup>, Edson Severnini<sup>1</sup>,  
Katharine G. Young<sup>11</sup>, Feng Zhao<sup>12</sup>

<sup>1</sup> Center for Earth System Science and Global Sustainability (CES<sup>3</sup>), Schiller Institute for Integrated Science and Society, Boston College, Chestnut Hill, MA 20467, USA

<sup>2</sup> College of Resources and Environment, Huazhong Agricultural University, Wuhan 430000, China

10 <sup>3</sup> Department of Earth and Environmental Sciences, Boston College, Chestnut Hill, MA 02467, USA

<sup>4</sup> Department of Engineering, Boston College, Chestnut Hill, MA 02467, USA

<sup>5</sup> School of Civil Engineering and Geomatics, Shandong University of Technology, Zibo 255000, China

<sup>6</sup> School of Computer Science and Technology, Harbin Institute of Technology, Harbin 150006, China

15 <sup>7</sup> Centro de Cambio Global UC, Dept. of Agricultural Economics, Pontificia Universidad Católica de Chile, Vicuña Mackenna 4860, Santiago 7820436, Chile.

<sup>8</sup> Graduate School of Global Environmental Studies, Sophia University, Tokyo 102-8554, Japan

<sup>9</sup> Department of History, Boston College, Chestnut Hill, MA 02467, USA

<sup>10</sup> Department of Geographical Sciences, University of Maryland, College Park, MD 20742, USA

<sup>11</sup> Boston College Law School, Boston, MA 02459, USA

20 <sup>12</sup> Key Laboratory of Sustainable Forest Ecosystem Management-Ministry of Education; College of Forestry, Northeast Forestry University, Harbin 150040, China

<sup>13</sup> National Key Laboratory of Smart Farm Technologies and Systems, Harbin, Heilongjiang 150006, China

*Correspondence to:* Hanqin Tian ([hanqin.tian@bc.edu](mailto:hanqin.tian@bc.edu))

25 **Abstract.** South America is a global hotspot for land use and land cover (LULC) change, marked by dramatic agricultural land expansion and deforestation. Developing high-resolution, long-term crop-specific data is essential for gaining a deeper understanding of natural-human interactions and addressing the impacts of human activities on regional biogeochemical, hydrological cycles, and climate. In this study, we integrated multi-source data, including high-  
30 resolution remote sensing data, model-based data, and historical agricultural census data, to



reconstruct the historical dynamics of four major commodity crops (i.e., soybean, maize, wheat, and rice) in South America at annual time scale and 1km×1km spatial resolution from 1950 to 2020. The results showed that cropland in South America has expanded rapidly through encroachment into other vegetation over the past 70 years. Specifically, soybean is one of the most dramatically expanded crops, increasing from essentially zero in 1950 to 48.8 Mha in 2020, resulting in a total loss of 23.92 Mha of other vegetation (i.e., forest, pasture/rangeland, and unmanaged grass/shrubland). In addition, the area of maize increased by a factor of 2.1 from 12.7 Mha in 1950 to 26.9 Mha in 2020, while rice and wheat areas remained relatively stable. The newly developed crop type data provide important insights for assessing the impacts of agricultural land expansion on crop production, greenhouse gas emissions, and carbon and nitrogen cycles in South America. Moreover, these data are instrumental for developing national policies, sustainable trade, investment, and development strategies aimed at securing food supply and other human and environmental objectives in South America and other regions. The datasets are available at <https://doi.org/10.5281/zenodo.14002960> (Xu et al., 2024).

## 1 Introduction

Land use and land cover (LULC) have changed dramatically under human activities, significantly affecting global biogeochemical and biophysical processes (Song et al., 2018; Tian et al., 2014; Foley et al., 2005). As one of the main types of LULC, cropland plays an



important role in supporting human nutritional needs, ensuring food security, and promoting  
50 economic development and social stability (He et al., 2017; Yu and Lu, 2017). However,  
cropland has encroached on other vegetation to meet the growing demand for food and fiber  
driven by population growth, consumption patterns, and other factors, accounting for about  
two-thirds of LULC changes from 1960 to 2019 (Winkler et al., 2021). Additionally, economic  
and policy factors have altered crop cultivation structure (Cheng et al., 2023; Song et al., 2021;  
55 Mueller and Mueller, 2010), which encompass a range of national, regional, and global  
pressures from trade, investment, and debt servicing, such as commodity and currency market  
volatility and market concentration (Boyd, 2023; Clapp, 2021). These changes may result in  
the transformation of crop types, which in turn reduces the resilience of agroecosystems, leads  
to biodiversity loss, and increases vulnerability to climate change (Renard and Tilman, 2019;  
60 Frison et al., 2011), in turn undermining food security and nutrition (IPCC, 2022). Therefore,  
understanding the spatial distribution and historical changes in crop types is crucial for  
quantifying the impacts of cropland expansion on ecosystems and climate.

Agriculture in South America has experienced significant changes driven by agricultural  
policies, socio-economic shifts, and technological innovations after the 1950s (Zalles et al.,  
65 2021; Ceddia et al., 2014; Altieri, 1992). These changes have not only reshaped regional  
economies, as in other historical periods of agrarian reform, but have also been justified by  
global food security goals, alongside such other important drivers as trade relationships,



investors, subsidies, and debt serving goals (OAS, 2024; Boyd, 2023). In this context, crop cultivation has shifted from traditional crops to high-yield and high-demand commodity crops, reflecting both the increasing global demand for food and fuel, as well as the urgent need to enhance agricultural efficiency and yields (Meyfroidt et al., 2014; Garrett et al., 2013). Specifically, the major commodity crops (i.e., maize, soybean, wheat, and rice) have become the core of agricultural production in South America (FAO, 2020). The cultivation of these crops has not only significantly boosted food production in the region, but also secured a strong position for many producers in the global food market. After the 1950s, countries in South America (e.g., Bolivia, Brazil, Chile, Colombia, Ecuador, and Peru) undertook land reforms to reduce land concentration and promote agricultural production (De Janvry et al., 1998), which significantly affected land use outputs and efficiency and laid a substantial foundation for the development of agriculture (De Janvry et al., 1998; Munoz and Lavadenz, 1997). After the 1980s, neoliberal economic reforms were further carried out in South America, accelerating the ongoing agricultural modernization (Chonchol, 1990) and greatly facilitating the cultivation of soybeans by eliminating price controls and export restrictions on agricultural products (Campos Matos, 2013). Since the 2000s, soybean has continued to grow dramatically due to global demand, technological advances, economic subsidies and other supportive policies (Song et al., 2021; de LT Oliveira, 2017). This growth has further bolstered the expansion of maize cultivation, driven by the promotion of maize-soybean cropping systems



and the adoption of direct seeding, no-tillage practices, and double cropping (Klein and Luna, 2022). In comparison, the area under wheat and rice cultivation has remained relatively stable. Although there is a growing demand for wheat, its market price is less fluctuating, leading  
90 farmers, farm managers, and investors to prefer crops with higher market returns (Erenstein et al., 2022). Meanwhile, rice primarily serves domestic demand rather than being export-oriented (Dawe et al., 2010). Despite government reports and documents that have recorded changes in the dynamics of agriculture in South America over the past few decades, there is still a lack of spatially explicit, long-time-series maps of historical crop types that reflect changes in crop  
95 distribution. This deficiency makes it difficult to fully understand the spatial and temporal evolution of major commodity crops and hinders understanding of their impacts on environmental changes.

Many efforts have produced commodity crop maps at regional or global scales. For example, datasets such as the Spatial Production Allocation Model (SPAM) (Yu et al., 2020),  
100 M3 (Monfreda et al., 2008), and CROPGRIDS (Tang et al., 2023) offer valuable solutions by providing detailed crop type information based on the census data and spatial allocation algorithms. SPAM, for instance, provides data on crop area, yield, and production for 42 major crops at a spatial resolution of 5 arcmin under four farming systems. However, these datasets have a coarse spatial resolution and are available for only a few years, which makes it  
105 challenging to accurately characterize the spatial-temporal distribution of crop types at finer



scales (Becker-Reshef et al., 2023; Ye et al., 2023). In contrast, with the continuous evolution of remote sensing technologies, high-resolution data were increasingly being used to develop fine-scale crop type maps. For example, Song et al. (2021) developed annually updated soybean maps with a 30 m resolution for South America from 2000 to 2023 using all Landsat  
110 and MODIS images and a probability sample of continental field observations. MapBiomass also provides high-resolution crop type maps for Argentina, Brazil, and Uruguay, covering the period from 1985 to the present (De Aballeyra et al., 2020; Petraglia et al., 2019; Souza and Azevedo, 2017). However, these existing datasets are available only at partial national or local scales, cover only a single crop type, or lack rigorous validation. Furthermore, most remote  
115 sensing data dates back only to 1985, making it challenging to depict crop dynamics further back. Therefore, it is imperative to develop high-resolution and long time-series crop type data for driving terrestrial ecosystem models to quantify the impact of crop dynamics on ecosystems and climate. Such a dataset will draw on innovations in earth science and data use to contribute to related fields that address the “advance of the agricultural frontier” in South America, and  
120 its implications for human-environmental interactions (OAS, 2024).

In this study, we aim to develop annual and 1-km crop-specific (i.e., soybean, wheat, maize, and rice) grid data for South America from 1950 to 2020 by integrating agricultural census data, and remote sensing-based and model-based crop type distribution maps. The structure of this paper includes three main sections. The first section provides a detailed



125 description of the input data and methods. The second section performs a comprehensive  
analysis of the spatial and temporal characteristics of four major commodity crops over the  
past seven decades. The third section compares the results of this study with other existing  
datasets and analyses the driving forces and uncertainties associated with the reconstructed  
data.

## 130 **2 Materials and method**

### **2.1 Study area**

This study aims to reconstruct crop type (i.e., soybean, wheat, maize, and rice) data at  
annual and 1 km resolution from 1950 to 2020 in South America using the high-resolution  
remote sensing-based crop type data, model-based crop type data, and historical agricultural  
135 census data. We focused on generating data for the 13 countries in South America, including  
Argentina (ARG), Bolivia (BOL), Brazil (BRA), Chile (CHL), Colombia (COL), French  
Guiana (GUF), Ecuador (ECU), Guyana (GUY), Paraguay (PRY), Peru (PER), Suriname  
(SUR), Uruguay (URY), and Venezuela (VEN) (Figure 1). Considering the data availability,  
we excluded the Falkland Islands and South Georgia and the South Sandwich Islands. We used  
140 GADM version 4.1 level 1 administrative units (i.e., province-level) as the basic unit for this  
study, which included a total of 243 administrative units (Table A1). Moreover, to maintain  
consistency with historical agricultural census data, some administrative units were regrouped



and merged for area calibration. Specifically, we merged Buenos Aires and Ciudad de Buenos Aires in Argentina; Bogotá D.C. and Cundinamarca in Colombia; Asunción and Central in  
145 Paraguay; Callao, Lima, and Lima Province in Peru; and all regions together in French Guiana. Ultimately, a total of 237 administrative units were used to reconstruct historical cropland density and crop type data (Table A1).

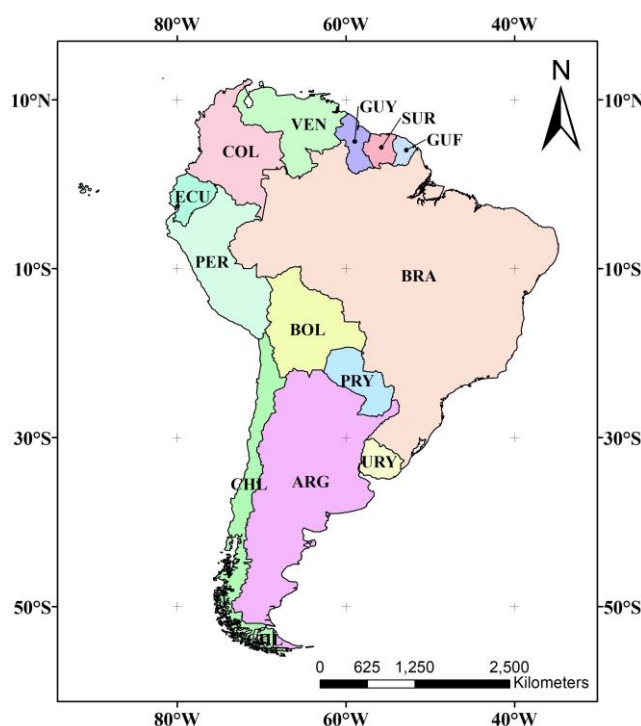


**Figure 1.** Countries in South America used in this study. ARG: Argentina; BOL: Bolivia; BRA: Brazil; CHL:  
150 Chile; COL: Colombia; GUF: French Guiana; ECU: Ecuador; GUY: Guyana; PRY: Paraguay; PER: Peru; SUR:  
Suriname; URY: Uruguay; VEN: Venezuela.





## 2.2 Input data

### 2.2.1 Gridded datasets and preprocessing

In this study, we used both remote sensing-based and model-based LULC and crop type  
 155 data to generate cropland density maps and crop type base map in South America. As shown  
 in Table 1, CGLS-LC100, GLC\_FCS30D, and HYDE 3.2 were used to generate cropland  
 density maps. SPAM 2010, GEOGLAM, GLAD, Argentina MNC, MapBiomass, and Uruguay  
 LC were used to generate base maps for crop types, and HILDA+ was used for land use  
 transition analysis.

160 **Table 1.** The datasets used in this study. C: cropland; M: maize; R: rice; S: soybean; W: wheat. For data sources,  
 please refer to Table S1.

Dataset	Resolution	Year range	Category used	Reference
CGLS-LC100	100 m, global Annual	2015 - 2019	C	(Buchhorn et al., 2020)
GLC_FCS30D	30 m, global 5-year interval (1985 - 2000) Annual (2000 - 2022)	1985 - 2022	C	(Zhang et al., 2024)
HYDE 3.2	5 arcmin, global 10-year interval	1950 - 2000	C	(Klein Goldewijk et al., 2017)
HILDA +	1 km, global Annual	1899 - 2019	8 categories	(Winkler et al., 2021)
SPAM 2010	5 arcmin, global	2010	M, R, S, W	(Yu et al., 2020)



GEOGLAM	0.05 degree, global	Integration of crop type data from 2010 to 2020	M	(Becker-Reshef et al., 2023)
GLAD	30 m, all major biomes where soybeans are cultivated in South America, annual	2020	S	(Song et al., 2021)
Argentina MNC	30 m, Argentina	2020	S, M, R	(De Abelleira et al., 2020)
MapBiomass	30 m, Brazil	2020	S	(Souza and Azevedo, 2017)
Uruguay LC	10 m, Uruguay	2018	R	(Petraglia et al., 2019)

Copernicus Global Land Service Land Cover Map (CGLS-LC100): CGLS-LC100 is a newly developed global LULC dataset with 100 m spatial resolution from 2015 to 2019, containing 23 land use types (Buchhorn et al., 2020). This product uses PROBA-V 100m time-series data and high-quality land cover training samples to construct a land cover classification model with 80% accuracy at Level 1. It has been compared to other popular LULC products and proven to perform better, making it a good choice for generating a base map for cropland density maps (Tsendbazar et al., 2019).

Global 30 m Land Cover Dynamics Monitoring Dataset (GLC\_FCS30D): GLC\_FCS30D is a global land cover product with a 30 m resolution based on continuous change detection algorithms (Zhang et al., 2024). It uses a detailed classification system containing 35 land cover



classes, covering the period from 1985 to 2022. The update cycle is 5 years before 2000 and annually after 2000. Moreover, it combines a continuous change detection algorithm, local  
175 adaptive classification models, and a spatial-temporal refinement method for dense time series to describe the land cover dynamics, verifying that the overall accuracy of the basic classification system for the 10 major land cover types exceeds 80%.

The History Database of the Global Environment (HYDE version 3.2): HYDE 3.2 uses a spatial allocation algorithm to generate spatially explicit maps from 10,000 BCE to 2017 CE  
180 by integrating historical statistical data with recent satellite information (Klein Goldewijk et al., 2017). It includes cropland (irrigated and rain-fed crops, and irrigated and rain-fed rice), grazing land (pasture and rangeland), and population maps with 5 arcmin spatial resolution. Numerous studies have demonstrated that HYDE 3.2 provides an excellent basis for reconstructing cropland density for historical periods (Li et al., 2023; Mao et al., 2023).

185 Historic Land Dynamics Assessment + (HILDA+): HILDA+ is a comprehensive global dataset designed to track changes in land use and cover from 1899 to 2019 at a spatial resolution of 1 km (Winkler et al., 2021). This dataset is notable for integrating multiple datasets, including high-resolution remote sensing data, land use reconstructions, and long-term statistical records. HILDA+ captures the dynamics of various land use categories, such as urban  
190 areas, cropland, pasture/rangeland, forests, unmanaged grass/shrublands, and areas with sparse or no vegetation.



Spatial Production Allocation Model (SPAM 2010): SPAM 2010 integrates high-resolution remote sensing data and agricultural statistics to generate a comprehensive product of crop area, yield, and production (Yu et al., 2020). This dataset enhances previous models by including data for 42 major crops under four different farming systems across a global 5 arc-minute grid. SPAM2010 addresses the limitations of administrative-level agricultural statistics by disaggregating them to a finer spatial resolution, thereby revealing the diversity and spatial patterns of agricultural production.

Group on Earth Observations Global Agriculture Monitoring (GEOGLAM): GEOGLAM is a global and up-to-date crop type map at 0.05-degree spatial resolution for four major commodity crops: wheat, maize, rice, and soybeans (Becker-Reshef et al., 2023). The development process involved extensive dataset selection and unification, considering factors such as seasonality, spatial resolution, accuracy, and data source specificity. These criteria ensure that the final maps are both accurate and useful for operational agricultural monitoring.

Global Land Analysis & Discovery (GLAD): GLAD provides soybean maps with a 30 m resolution for South America covering the period from 2000 to 2023 (Song et al., 2021). The products were derived by integrating all Landsat and MODIS images captured during the growth stage of soybeans. GLAD soybeans maps cover all major biomes in South America (i.e., Pampas, Chiquitania, Chaco, Cerrado, Atlantic Forest, Amazonia, and the Pantanal and Caatinga biomes). Validated using a probability sample of field observations across the



continent, the GLAD soybean maps have an overall accuracy exceeding 94% with both high user's and producer's accuracies.

MapBiomass provides land use and land cover maps with a 30 m resolution for Argentina, Brazil, and Uruguay, which include the major land use and cover types, as well as some crop-specific information (e.g., soybean and rice). Argentina MNC provides detailed crop type maps (e.g., soybean, maize, and rice) with a 30 m resolution for Argentina from 2018 to 2022 (De Abelleira et al., 2020). The data was generated by supervised classification of Landsat-8 observations using a random forest classifier to independently classify different agricultural zones, achieving an overall accuracy exceeding 80% for both summer and winter crops. MapBiomass Brazil was generated using all available Landsat observations covering from 1985 to 2022 and processed in Google Earth Engine, achieving an overall accuracy of around 80% in most biomes at Level 1 (Souza and Azevedo, 2017). Integrated Land Cover/Use Map of Uruguay (Uruguay LC) was also generated in 10 m resolution with crop-specific information in 2018 (Petraglia et al., 2019).

To reconstruct the historical cropland and crop type dynamics, all datasets needed to be preprocessed. First, the high-resolution datasets (i.e., CGLS-LC100, GLC\_FCS30D, GLAD, Argentina MNC, MapBiomass, and Uruguay LC) were aggregated to a 1 km resolution to attain the fractional cropland and crop type. Second, HYDE3.2, SPAM2010, and GEOGLAM were resampled to 1 km spatial resolution using the bilinear method. Finally, the projection of all



230 datasets was transformed to WGS84 for further analysis, with all processes carried out in Google Earth Engine.

### 2.2.2 Inventory datasets

The inventory datasets were collected at three levels: national, provincial, and municipal. The national data mainly come from the Food and Agriculture Organization (FAO), while the provincial and municipal data primarily come from agriculture censuses released by  
 235 governments (Table 2). Eventually, a total of 136 provincial-level statistics on LULC and crop-specific information from 13 countries were collected and sorted to reconstruct historical crop-specific areas at the provincial level. Additionally, 10 municipal-level statistics were used to evaluate the crop-specific maps generated in this study.

240 **Table 2.** The inventory datasets used in this study. NAT: National; PRO: Provincial; MUN: Municipal; C: cropland; M: maize; R: rice; S: soybean; W: wheat; P: Production. CNA: National Agricultural Census; INDEC, INE, IBGE, and INE are the national statistics and census bureaus of the corresponding countries. Due to the large number of data sources, detailed information is provided in Table S1.

Country	Resolution	Year range	Category	Source
Argentina	PRO, MUN	1960 - 2018	C, M, R, S, W	INDEC
	5- to 10-year interval			CNA
Bolivia	PRO	1950 - 2020	M, R, S, W	INE
	Annual (1984 -2022)			CNA
	PRO			1950, 1984, 2013
	MUN	1950	C, M, R, S, W	
Brazil	PRO	1940 - 2006	P	IBGE
	5- to 10-year interval			CNA
	PRO	1970 - 2017	C, M, R, S, W	



5- to 10-year interval				
	MUN	1995, 2017	C, M, R, S, W	
Chile	PRO	1997 - 2020	C, M, R, S, W	INE CNA
	10-year interval			
	MUN	2007	C, M, R, S, W	
Colombia	PRO	1960 - 2019	C, M, R, S, W	CNA
	5-year interval (1996 - 2011)			
	Annual (2011 - 2019)			
	MUN	1960	M, R	
Ecuador	PRO	1995 - 2020	C, M, R, S, W	CNA
	10-year interval			
Guyana	CNT	1960 - 2016	R	CNA
	Annual			
	PRO	1994 - 2016	R	
Annual (2007 - 2016)				
Paraguay	PRO	2008, 2020	C	
	PRO	1991 - 2020	M, R, S, W	CNA
	Annual (2000 - 2022)			
Peru	PRO	1929, 1993	M, R, S, W	CNA
	PRO	2012	C	
Suriname	PRO	1995, 2008	M, R, S, W	CNA
	PRO	2008	C	
Uruguay	PRO	1990, 2000	M, R, S, W	CNA
Venezuela	PRO	1995	M, R	CNA
Global	NAT	1961 - 2020	C, M, R, S, W	FAO

### 2.3 Generating cropland density maps

245 We used both grided and inventory datasets to generate cropland density maps at a resolution of  $1 \text{ km} \times 1 \text{ km}$ , covering the period from 1950 to 2020 (Figure 2). Specifically,



the reconstruction process consists of the following steps: (1) the total cropland area was reconstructed from 1950 to 2020 at the provincial level (Table 2, Equation 1). We utilized trends from national-level data to reconstruct provincial cropland areas for years with missing values. From 1961 to 2020, we used FAO data. For years before 1961, we relied on national-level agricultural census data for some countries, while for countries with no data available before 1961, we used HYDE data. Then, the linear interpolation method was used to generate the annual total cropland area at the provincial level. In this process, we assume that the inter-annual rate of change in cropland areas is consistent at both the provincial and national levels. Since the data years differ among countries, we performed the reconstruction on a country-by-country basis. (2) Second, we generated the potential cropland density maps with a resolution of  $1 \text{ km} \times 1 \text{ km}$  from 1950 to 2020. Based on the definitions of various datasets and a comparison of total cropland area at the provincial level, we selected CGLS-LC100, GLC FCS30D, and HYDE as sources to generate potential cropland density maps (Table A1 & A2 & Figure A1). Since CGLS-LC100 and the reconstructed cropland area exhibit high agreement at the provincial level ( $R^2 = 0.92$ ,  $RMSE = 0.46 \text{ Mha}$ ), we choose CGLS-LC100 as the baseline data for generating the potential cropland density maps. We first aggregated the CGLS-LC100 to 1 km resolution for 2015-2019 and kept the 2019 values for 2020. Then, we used the aggregated CGLS-LC100 in 2015 as a base map to generate the potential cropland density maps for the period from 1985 to 2014 by using the annual changes derived from the resampled





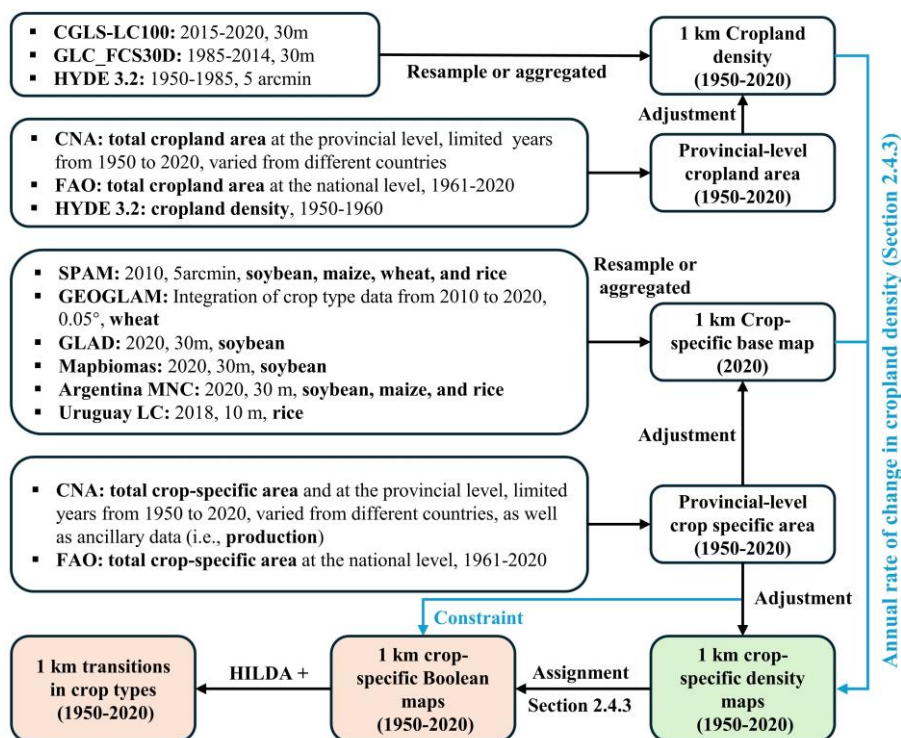
GLC FCS30D cropland density. Similarly, the cropland density maps for the period from 1950 to 1985 were generated using the decadal changes derived from the resampled HYDE cropland density. Finally, we filled the years with missing values based on linear interpolation on a grid-by-grid basis. (3) Third, we adjusted the potential cropland density maps using reconstructed provincial-level cropland area to obtain an annual cropland density map between 1950 and 2020 (Equation 2). If the cropland density of a grid is less than 0 or greater than 1, we assign it a value of 0 or 1, respectively. This adjustment process is repeated until the difference between the adjusted area and the total cropland area at the provincial level is less than 100 ha.

$$CropArea_{c,s,i} = CropArea_{c,s,i+j} \times \frac{Reference\ data_{c,i}}{Reference\ data_{c,i+j}} \quad (1)$$

where,  $CropArea_{c,s,j}$  and  $CropArea_{c,s,i+j}$  are the reconstructed cropland area of province  $s$  in country  $c$  in year  $i$  and  $i + j$ ;  $Reference\ data_{c,i}$  and  $Reference\ data_{c,i+j}$  are the reference values for the total cropland area in country  $c$  in year  $i$  and  $i + j$ , respectively. Between 1961 and 2020, the value of  $j$  is 1; While before 1961, the value of  $j$  corresponds to the year difference in the reference data.

$$Grid'_k = Grid_k + \frac{(TotalArea - \sum_1^n Grid_k)}{n} \quad (2)$$

where,  $Grid'_k$  is the adjusted cropland density for the  $k$ th grid,  $Grid_k$  is the potential cropland density,  $TotalArea$  is the reconstructed cropland area at the provincial level, and  $n$  is the total number of valid crop grids (cropland density  $> 0$ ) in a province.



285 **Figure 2.** The flow chart in this study. CNA refers to Census National Agriculture.

## 2.4 Generating gridded crop-specific maps

### 2.4.1 Building crop-specific base map for the year 2020

We set 2020 as the base year and generated the base map of four commodity crops (i.e.,  
 290 maize, rice, soybean, and wheat) by integrating multiple remote sensing-based and model-  
 based datasets. First, considering that high-resolution crop distribution maps do not cover the  
 whole of South America, we used the resampled SPAM2010 data to generate the initial base



map. We then replaced the corresponding regions with higher-resolution data available for  
around 2020. Specifically, the base map for maize was generated from Argentina MNC (2020)  
295 and SPAM (2010). The base map for soybean was generated from Argentina MNC (2020),  
MapBiomass (2020), GLAD (2020), and SPAM (2010). The base map for rice was generated  
from Uruguay LC (2018), Argentina MNC (2020), and SPAM (2010). The base map for wheat  
was generated from GEOGLAM (2020). Finally, we used reconstructed crop-specific  
harvested area in 2020 at the provincial level to further adjust the base map (Section 2.4.2,  
300 Equation 2).

#### **2.4.2 Reconstructing the annual crop-specific harvested area at the provincial level**

Long-term historical crop-specific harvested areas at the provincial level were  
reconstructed from 1950 to 2020 using multiple sources of historical inventory data (Table 2).  
The detailed reconstruction processes are described below. First, the time series of crop-  
305 specific harvested areas at the provincial level were obtained from the National Agricultural  
Census (CNA), the national statistics office (e.g., INDEC, IBGE, and INE, etc), and literature.  
Second, anomaly values in the time series of the crop-specific harvested area were removed  
after cross-referencing with time series trend and national level data, based on the assumption  
that the crop-specific harvested area exhibits a gradual upward or downward trend. Third, the  
310 FAO trend was used to fill the gaps between 1961 and 2020 (Equation 1). Fourth, countries  
lacking statistics data were reconstructed using production, due to the strong correlation



between production and harvested area ( $R^2 = 0.92$ , Equation 3). For example, we collected crop production data as a reference to reconstruct crop-specific harvested areas at the provincial level in Brazil for the period from 1950 to 1970. For countries with no available data before  
315 1961, we maintain consistency by using the data from 1961. Finally, the liner interpolation was used to fill the crop-specific harvested area with the missing values.

$$CTArea_{c,s,i} = CTArea_{c,s,i+j} \times \frac{Prod_{c,s,i}}{Prod_{c,s,i+j}} \quad (3)$$

where,  $CTArea_{c,s,j}$  and  $CTArea_{c,s,i+j}$  are the reconstructed crop-specific harvested area of province  $s$  in country  $c$  in year  $i$  and  $i + j$ ;  $Prod_{c,s,i}$  and  $Prod_{c,s,i+j}$  are the crop production of  
320 province  $s$  in country  $c$  in year  $i$  and  $i + j$ .

### 2.4.3 Spatializing provincial-level data to generate annual crop-specific maps

The reconstructed crop-specific harvested area at the provincial level was spatially allocated to the grid level based on the generated crop-specific base map and annual cropland density to obtain 1 km crop-specific maps from 1950 to 2020. Specifically, we took 2020 as  
325 the baseline and used the ratio of cropland density between two adjacent years to obtain the density of the crop-specific harvested area in the previous year (Equation 4). We assumed that the inter-annual trend in crop-specific harvested area is consistent with the trend in area changes in cropland density. To ensure that the allocated area is consistent with the total harvested area



at the provincial level, we further adjusted the allocated crop-specific harvested area using  
330 Equation 2.

$$CTDensity_{k,i-1} = \frac{CropDensity_{k,i-1}}{CropDensity_{k,i}} \times CTDensity_{k,i} \quad (4)$$

where,  $CTDensity_{k,i-1}$  and  $CTDensity_{k,i}$  are the density of crop-specific harvested area for the  
kth grid in years  $i$  and  $i-1$ ;  $CropDensity_{k,i-1}$  and  $CropDensity_{k,i}$  are the cropland density for the  
kth grid in years  $i$  and  $i-1$ .

335 To analyze the transitions between land use/cover and crop-specific maps, we further  
transformed the crop type density data into Boolean data. Specifically, we first sorted the grids  
by crop type density and then assigned Boolean values to the top N grids until the final area  
differed from the reconstructed provincial-scale area by less than 100 ha. We proceed in the  
order of soybean, maize, wheat, and rice. Finally, we obtained annual Boolean data on crop  
340 types from 1950 to 2020.

## 2.5 Accuracy assessment

We performed accuracy assessments using three strategies: (1) comparing crop-specific  
areas derived from existing gridded products with those from this study at the provincial level.  
To ensure the reliability of the assessment, we used data from years not included as inputs,  
345 serving as an independent reference for the evaluation (i.e., MapBiomass (2000, 2005, and  
2010), SPAM (2000 and 2005), GEOGLAM (2020), GLAD (2005 and 2010), and Brazil



Conba (2017 – 2020, Table S1)). (2) validating reconstructed crop-specific maps in this study with crop-specific areas collected from agricultural censuses at the municipal level. (3) performing visual comparisons using existing remote sensing-based high-resolution data (Argentina MNC, GLAD, Uruguay LC, and WorldCereal) at the grid level. This process is primarily evaluated by calculating the difference between the fraction of our developed data and the fraction of other datasets within each grid. Given the limited availability of high-resolution data, we began by comparing data from around 2020 (i.e., Argentina MNC (2020), Uruguay LC (2018), and WorldCereal (2021)). Additionally, GLAD data (2001, 2010, and 2020) were used for long-term series comparisons. For evaluation at the provincial and municipal levels, we used the coefficient of determination ( $R^2$ , Equation 5), Normalized Root Mean Square Error ( $nRMSE$ , Equation 6), and *slope* (Equation 7) to quantify the performance of our developed crop-specific data relative to other datasets. Higher  $R^2$  values, lower  $nRMSE$ , and *slope* closer to 1 indicate better agreement between actual and estimated crop-specific areas, and vice versa.

$$R^2 = 1 - \frac{\sum_{i=1}^n (x_i - y_i)^2}{\sum_{i=1}^n (x_i - \bar{x})^2} \quad (5)$$

$$nRMSE = \frac{\sqrt{\frac{1}{n} \sum_{i=1}^n (x_i - y_i)^2}}{\bar{x}} \quad (6)$$

$$Slope = \frac{\sum_{i=1}^n (x_i - \bar{x})(y_i - \bar{y})}{\sum_{i=1}^n (x_i - \bar{x})^2} \quad (7)$$



Where  $n$  represents the number of samples;  $x_i$  and  $y_i$  are the actual and estimated crop-specific  
365 areas for the  $i$ th sample; and  $\bar{x}$  and  $\bar{y}$  represent the average of the actual crop-specific areas.

### 3 Results

#### 3.1 Dynamics of crop types from 1950 to 2020 in South America

Figure 3 shows the spatial pattern of soybean, wheat, maize, and rice from 1950 to 2020  
in South America. Overall, there has been a significant increase over time in the area and  
370 density of cultivation for all major crops. Soybean and maize have expanded significantly in  
Argentina and Brazil. Specifically, soybean was practically not cultivated in South America in  
1950, with small amounts starting to appear in 1980. After 2000, soybean cultivation increased  
significantly, covering large areas in central and southern Brazil and central Argentina. Maize  
was initially cultivated mainly in central Argentina, southern Brazil, and northern Colombia  
375 and Venezuela. The extent and density of maize cultivation gradually increased, showing a  
trend of expansion from south to north. Rice is cultivated in a relatively small area in South  
America, mainly in Uruguay, northern parts of Colombia and Venezuela, and in the Brazilian  
states of Maranhão, Tocantins, and Rio Grande do Sul. Except for an increase in the extent of  
cultivation around 1980, there has been relatively little change in the rest of the years. Wheat  
380 is more concentrated in southern South America, including the provinces of Buenos Aires,  
Córdoba, and Santa Fe in Central Argentina; Rio Grande do Sul in southern Brazil; and

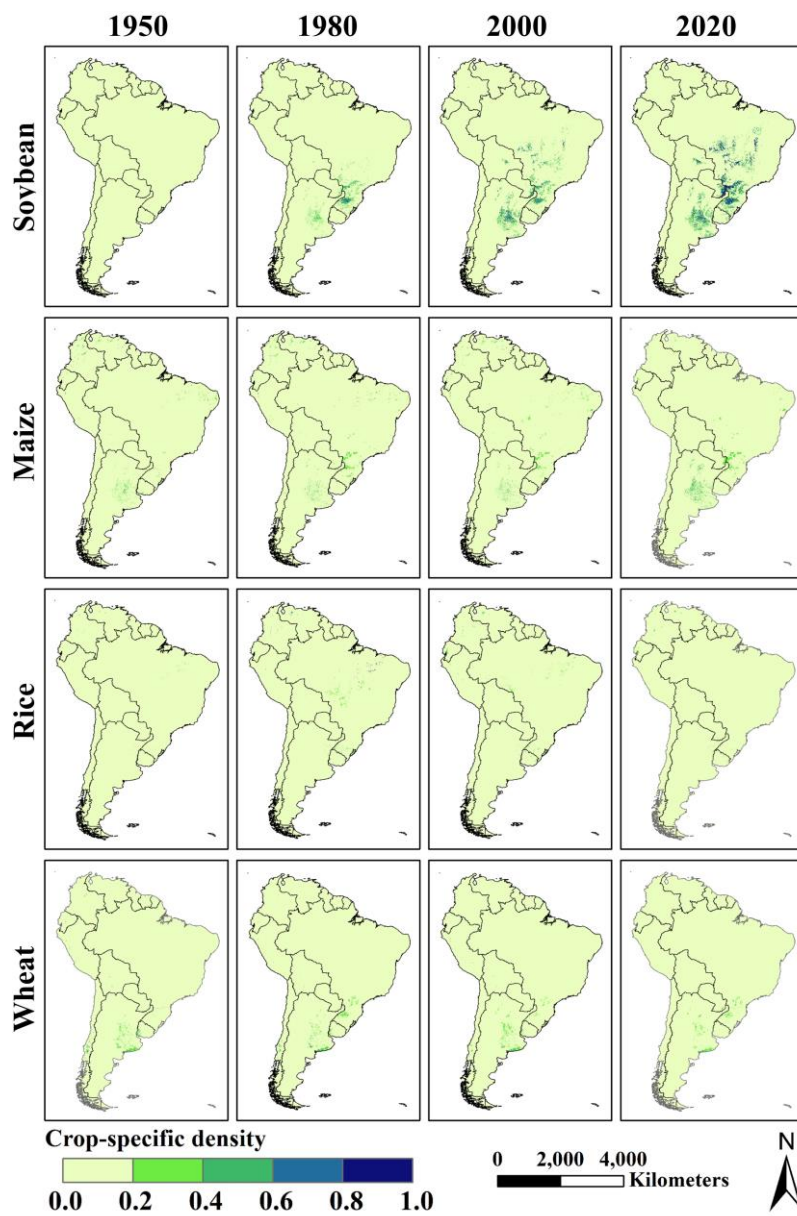


Araucanía, Biobío in central Chile. Between 1950 and 2020, the extent of wheat cultivation has remained relatively stable. Additionally, we calculated the changes in the total area of different crops in different countries and the entire South America (Figure 4 & Figure A2).

385 Soybean is the crop with the most rapid change in the area, growing from 0.08 Mha in 1950 to 48.8 Mha in 2020, an increase of 610 times. The area of maize showed a slow growth trend until 2000, increasing from 12.7 Mha in 1950 to 16.5 Mha in 2000. Since 2000, the growth rate has gradually increased, reaching a total area of 26.9 Mha in 2020, with an average annual growth rate of 6.8 times higher than that of the pre-2000 period. The area of rice increased

390 gradually before 1980, growing from 3.2 Mha in 1950 to 6.7 Mha in 1980, followed by a gradual decline, falling back to 3.8 Mha by 2020. In contrast, wheat is relatively stable, increasing slightly from 7.6 Mha in 1950 to 7.9 Mha in 2020. At the country level, Brazil has the largest area of soybean, maize, and rice, while Argentina has the largest area of wheat.





395 **Figure 3.** The spatial pattern of soybean, maize, rice, and wheat from 1950 to 2020. The first, second, third, and fourth rows represent the crop-specific fraction of soybean, maize, rice, and wheat.

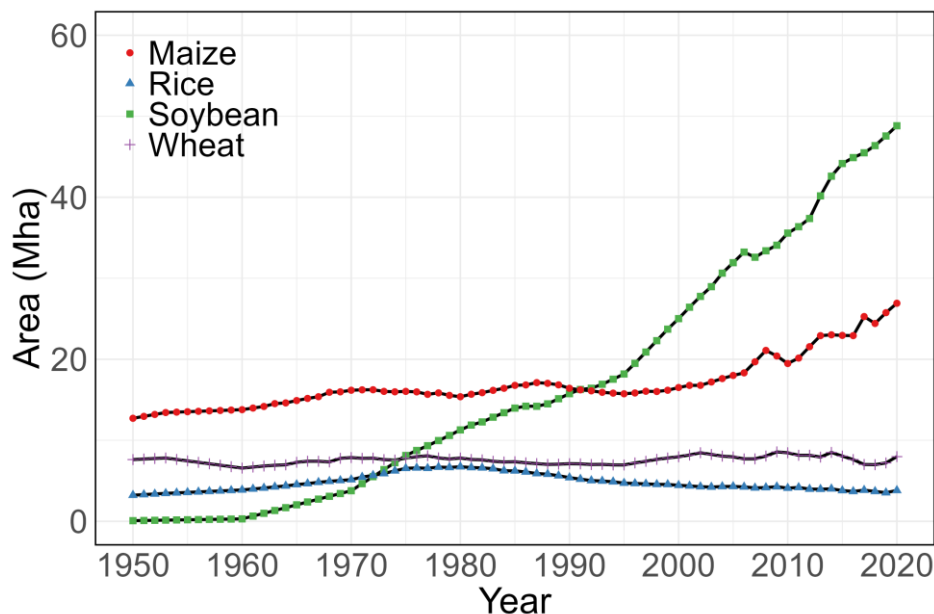


**Figure 4.** Temporal changes in crop-specific areas in South America during 1950-2020.

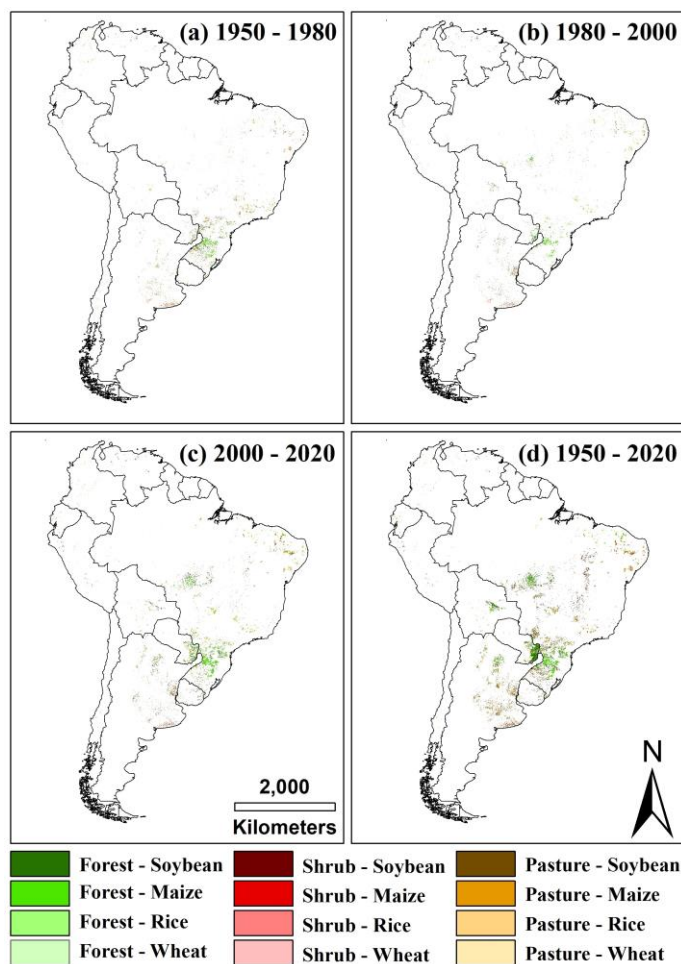
### 3.2 Transitions in crop types

400 Transition analysis can help us understand the underlying conversions of cropland expansion, and how these transition characteristics can be used to guide future crop cultivation. Therefore, we performed transition analysis by overlaying our reconstructed crop type maps with land use data from HILDA+. Over the past 70 years, soybean and maize have expanded dramatically through encroachment on other vegetation, including forest, pasture/rangeland, and unmanaged grass/shrubland (Figure 5 & Table 3). Specifically, 24.49 Mha of the forest was converted to the four major crops. Additionally, 13.82 Mha of pasture/rangeland, 11.26 Mha of unmanaged grass/shrubland, and 0.20 Mha of sparse/no vegetation were also converted.

405



Most of this conversion was to soybean, accounting for 23.92 Mha, which represents 48.1 % of the total converted area. Regarding crops, different types exhibit varying extents of spatial expansion and encroachment on other vegetation. The total area of soybean encroaching upon forest, pasture/rangeland, and unmanaged grass/shrubland was 12.26 Mha, 5.26 Mha, and 6.39 Mha, respectively. The growth rate of encroachment upon forests increased rapidly from 0.05 Mha/year in 1950-1980 to 0.32 Mha/year in 2000-2020. In terms of spatial distribution, soybean encroachment occurred mainly in the Brazilian provinces of Mato Grosso, Paraná, and Rio Grande do Sul, as well as southeastern Paraguay and central Bolivia for forests; in eastern Argentina and parts of Brazil for pasture/rangeland; and at the confluence of the provinces of Maranhão, Piauí, and Bahia for grasslands. On the other hand, the total area of maize encroachment from forest, pasture/rangeland, and unmanaged grass/shrubland was 9.22 Mha, 5.44 Mha, and 3.57 Mha, respectively. The growth rate of encroachment from forests increased from 0.13 Mha/year in 1950-1980 to 0.36 Mha/year in 2000-2020. The spatial pattern of maize encroachment was similar to that of soybean. The expansions of other crops are smaller in area compared to soybeans and maize, and more dispersed in their spatial distribution. Overall, cropland expansion led to significant reductions in other vegetation, with the most dramatic increase occurring in staple crops, particularly soybean and maize.



425

**Figure 5.** Spatial pattern of transitions between LULC and crop-specific areas from 1950 to 2020. (a) 1950 – 1980; (b) 1980 – 2000; (c) 2000 – 2020; (d) 1950 – 2020. Pasture: pasture/rangeland; Shrub: unmanaged grass/shrubland.

430



**Table 3.** Statistics of transition areas in South America from 1950 to 2020 (Unit: Mha).

Transition types		1950 - 1980	1980 - 2000	2000 - 2020	1950 - 2020
Past	Present				
Forest	Soybean	1.43	1.92	6.47	12.26
	Maize	4.00	3.07	7.26	9.22
	Wheat	1.14	0.38	1.16	1.76
	Rice	1.11	0.88	0.80	1.25
	<b>Sub-total</b>	<b>7.68</b>	<b>6.25</b>	<b>15.69</b>	<b>24.49</b>
Pasture/rangeland	Soybean	0.87	1.00	2.81	5.26
	Maize	3.35	2.94	5.04	5.44
	Wheat	1.75	1.27	1.59	2.08
	Rice	1.30	1.34	1.30	1.04
	<b>Sub-total</b>	<b>7.27</b>	<b>6.55</b>	<b>10.74</b>	<b>13.82</b>
Unmanaged grass/shrubland	Soybean	0.92	0.49	1.03	6.39
	Maize	2.00	0.82	1.76	3.57
	Wheat	1.07	0.64	0.59	0.91
	Rice	0.99	0.14	0.25	0.39
	<b>Sub-total</b>	<b>4.98</b>	<b>2.09</b>	<b>3.63</b>	<b>11.26</b>
Sparse/no vegetation	Soybean	0.00	0.00	0.00	0.01
	Maize	0.10	0.07	0.08	0.12
	Wheat	0.01	0.01	0.01	0.01
	Rice	0.02	0.02	0.03	0.06
	<b>Sub-total</b>	<b>0.13</b>	<b>0.10</b>	<b>0.12</b>	<b>0.20</b>



### 435 3.3 Evaluation of the crop-specific maps

#### 3.3.1 Evaluation against existing datasets at the provincial level

We compared the crop-specific areas (i.e., soybean, wheat, maize, and rice) derived from existing datasets with the crop-specific maps developed in this study at the provincial level. The datasets include MapBiomass (soybean and rice in 2000, 2005, and 2010), SPAM (soybean, 440 wheat, maize, and rice in 2000 and 2005), GEOGLAM (soybean, maize, and rice), GLAD (soybean in 2005 and 2010), and Brazil Conba (soybean and rice from 2017 to 2020). The soybean areas from this study are consistent with Brazil Conba (Figure 6a:  $R^2 = 1$ , slope = 1.38) and SPAM ( $R^2 = 0.96$ , slope = 1.15) but lower than those from MapBiomass ( $R^2 = 0.99$ , slope = 1.41), GEOGLAM ( $R^2 = 0.92$ , slope = 1.49), and GLAD ( $R^2 = 0.91$ , slope = 1.56). The wheat 445 areas from this study are consistent with SPAM (Figure 6b:  $R^2 = 0.93$ , slope = 1.15). The maize areas from this study are generally consistent with SPAM (Figure 6c:  $R^2 = 0.94$ , slope = 1.01). However, they differ significantly from those of GEOGLAM ( $R^2 = 0.65$ , slope = 3.36). For rice, the areas from this study match well with Brazil Conba (Figure 6d:  $R^2 = 1$ , slope = 1.93) and SPAM ( $R^2 = 0.87$ , slope = 1.15), but differ significantly from those of GEOGLAM ( $R^2 =$  450  $0.70$ , slope = 0.83) and MapBiomass ( $R^2 = 0.66$ , slope = 0.55). Generally, the crop-specific areas reconstructed in this study were consistent with other datasets, with most  $R^2$  values exceeding 0.87 (Figure 6), except for maize and rice in GEOGLAM and wheat in MapBiomass. This suggests that our method is reliable in reconstructing crop-specific areas at the provincial level



despite some discrepancies. These discrepancies may be attributed to variations in data sources,  
 455 processing methods, or classification criteria.

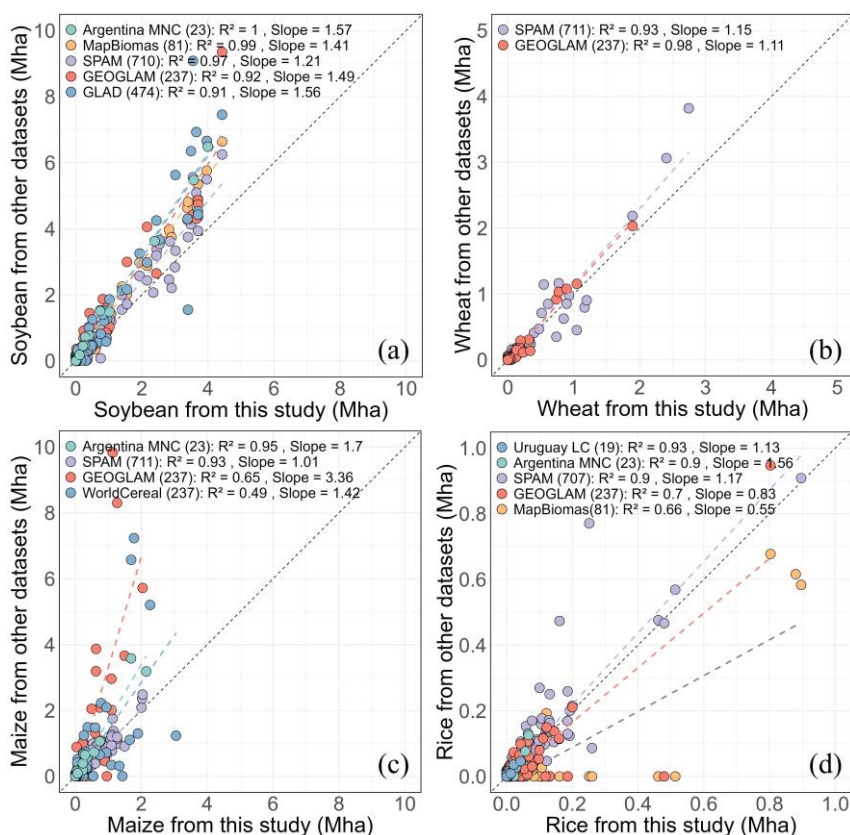


**Figure 6.** Comparison of crop type areas between this study and existing datasets (i.e., Argentina MNC, MapBiomias, SPAM, GEOGLAM, GLAD, WorldCereal, and Uruguay LC) at the provincial level. (a) Soybean; (b) Wheat; (c) Maize; (d) Rice. The numbers in parentheses represent the total number of samples.

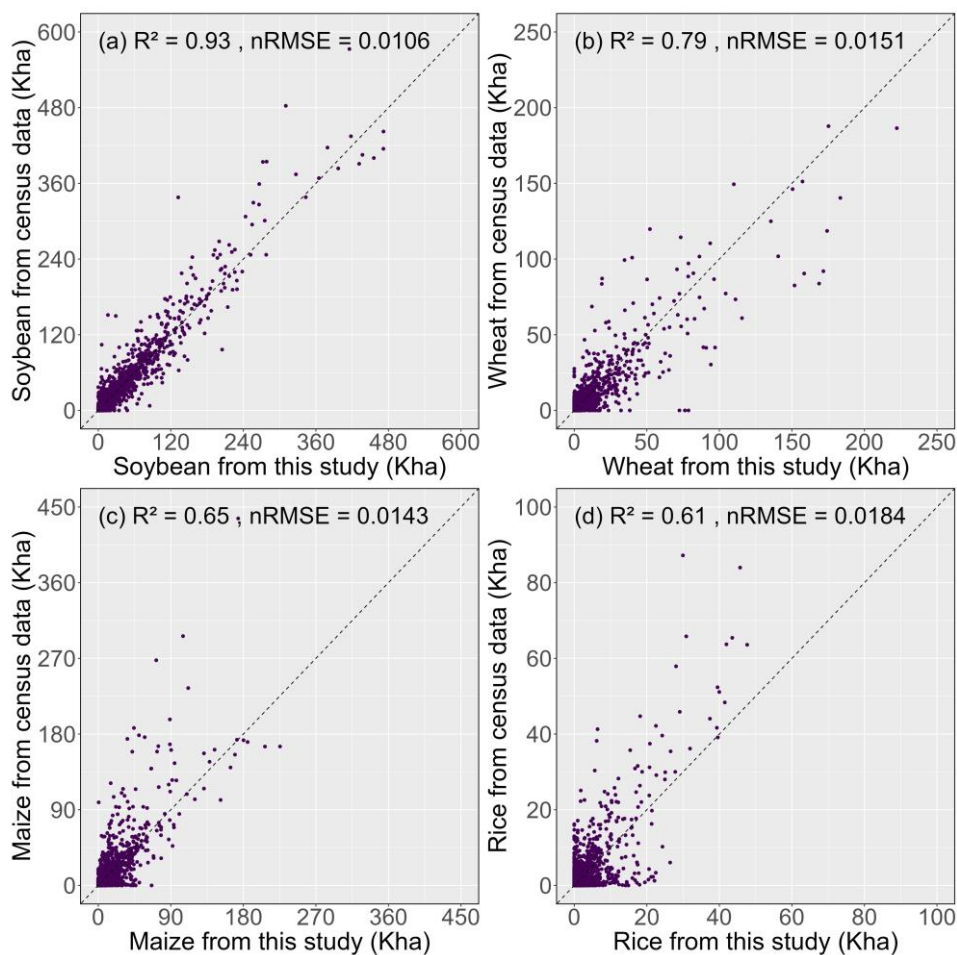
### 460 3.3.2 Evaluation using inventory data at the municipal level

To ensure the effectiveness of the evaluation, we collected crop type areas from various countries across different years at the municipal level to evaluate our reconstructed crop type



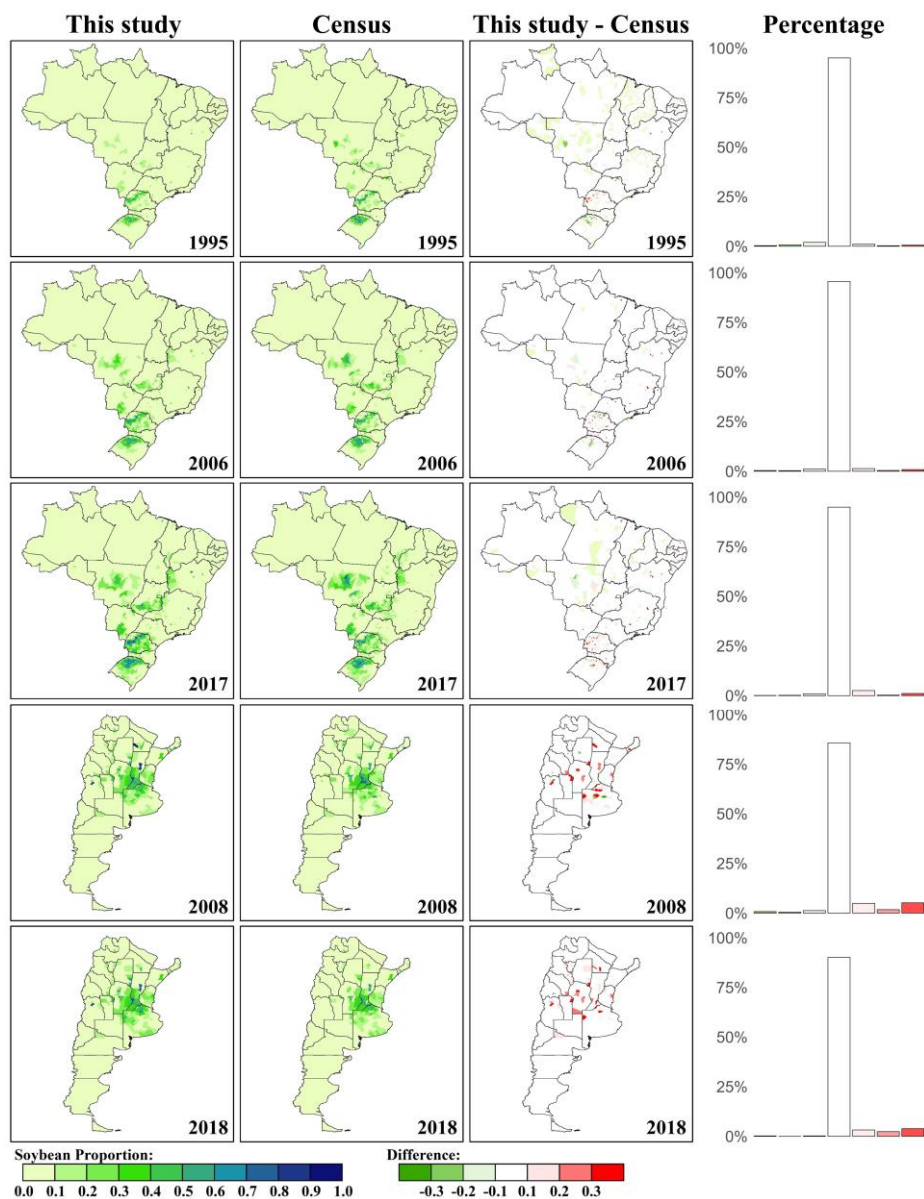
maps (Argentina: 1960, 2008, and 2018; Bolivia: 1950; Brazil: 1995, 2006, 2017; Chile: 2017; Colombia: 1960; Paraguay: 2008). Figure 7 shows the comparison results of crop-specific areas  
465 for soybean, wheat, maize, and rice at the municipal level between census data and this study. We used  $R^2$  and  $nRMSE$  to quantify the precision and reliability of our data. Specifically, the soybean and wheat areas derived from this study fit well with those from census data (soybean:  $R^2 = 0.93$ ,  $nRMSE = 0.0106$ ; wheat:  $R^2 = 0.79$ ,  $nRMSE = 0.0151$ ), whereas the performance of the maize and rice is relatively less accurate (maize:  $R^2 = 0.65$ ,  $nRMSE = 0.0143$ ; rice:  $R^2 =$   
470  $0.61$ ,  $nRMSE = 0.0184$ ). Additionally, the spatial pattern of soybean, maize, wheat, and rice proportions (i.e., crop-specific area/municipal area) is consistent with the census data (Figure 8 & Figure A3-A5). Soybean cultivation in Brazil is concentrated in the southern and central regions, and the soybean proportions derived from this study are relatively close to the census data, with minor over- and underestimates in only a few areas, such as Paraná and Rio Grande  
475 do Sul. On the other hand, Argentina shows a similar geographical distribution pattern, with the main cultivation areas concentrated in the central region, but with overestimation in some areas. The main concentration is in the provinces of Córdoba and Buenos Aires. The areas for the remaining three crops (i.e., maize, wheat, and rice) are in good agreement with the census data, except for Brazilian maize in 2017, which is slightly underestimated in central Brazil.





480

**Figure 7.** Comparison of the crop-specific areas between this study and census data at the municipal level. (a) soybean; (b) wheat; (c) maize; (d) rice. The municipal-level inventory data used include Argentina (1960, 2008, and 2018), Bolivia (1950), Brazil (1995, 2006, and 2017), Chile (2017), Colombia (1960), and Paraguay (2008).



485 **Figure 8.** Spatial comparison of the soybean proportion (i.e., soybean area/municipal area) between this study and census data at the municipal level in Argentina (2008 and 2018) and Brazil (1995, 2006, and 2017). Left column: soybean proportion from this study; Middle column: soybean proportion from census data; Right column: the difference in soybean proportion between this study and census data.



### 3.3.3 Evaluation using satellite-based datasets at the grid level

490 We also compared satellite-based crop type maps with our reconstructed data at the grid level. Due to the lack of crop type maps for the entire South America, we used Argentina MNC and Uruguay LC as baselines for the comparison of soybean, wheat, and maize. However, some maps generated by satellite data do not distinguish wheat from winter cereals (Van Tricht et al., 2023), so we used the resampled GEOGLAM as the baseline for the comparison of wheat.

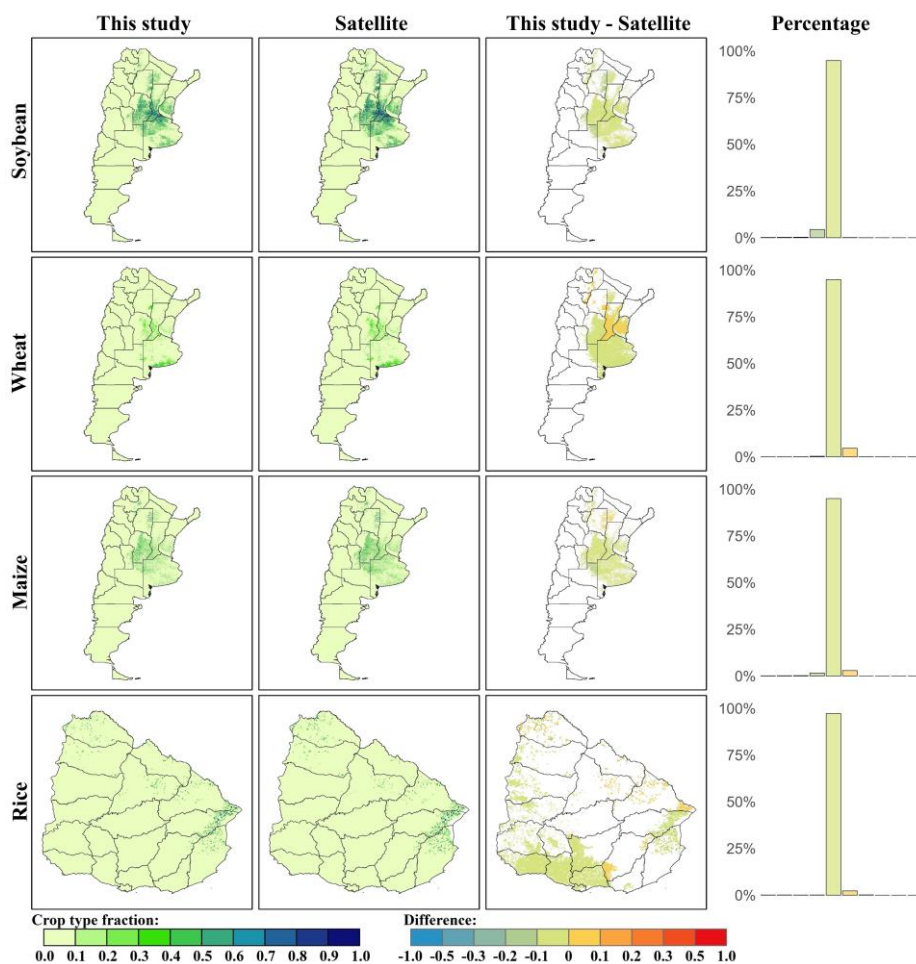
495 Figure 9 shows the spatial comparison of soybean, wheat, maize, and rice between satellite-based data and reconstructed data at the grid level. The results of the estimation of the proportion of soybean, wheat, maize, and rice cultivation show high agreement with the satellite data in terms of spatial distribution. However, there were slight over- or under-estimates in some areas, especially in regions with concentrated crop cultivation. The

500 percentage histograms provide detailed information on the distribution of differences, with most of the differences being less than 10 %, indicating that the estimation results of this study are generally reliable. Since most satellite-based crop maps are from around 2020 and are used as base maps to reconstruct historical crop distributions, we used soybean time-series data from GLAD to further assess the reliability of our reconstructed data. We chose 2001, 2010, and

505 2020 for comparison, with only the 2020 data used to construct the base map in Section 2.4.1. As shown in Figure 10, the estimates from this study also show high agreement with the GLAD



data in terms of spatial distribution for 2001, 2010, and 2020, with differences of less than 10 %.



510 **Figure 9.** Spatial comparison of soybean, wheat, maize, and rice maps between satellite-based high-resolution data and the reconstructed data from this study. The soybean and maize maps are from Argentina MNC, the rice map is from Uruguay LC, and the wheat map is from GEOGLAM due to the lack of high-resolution data.

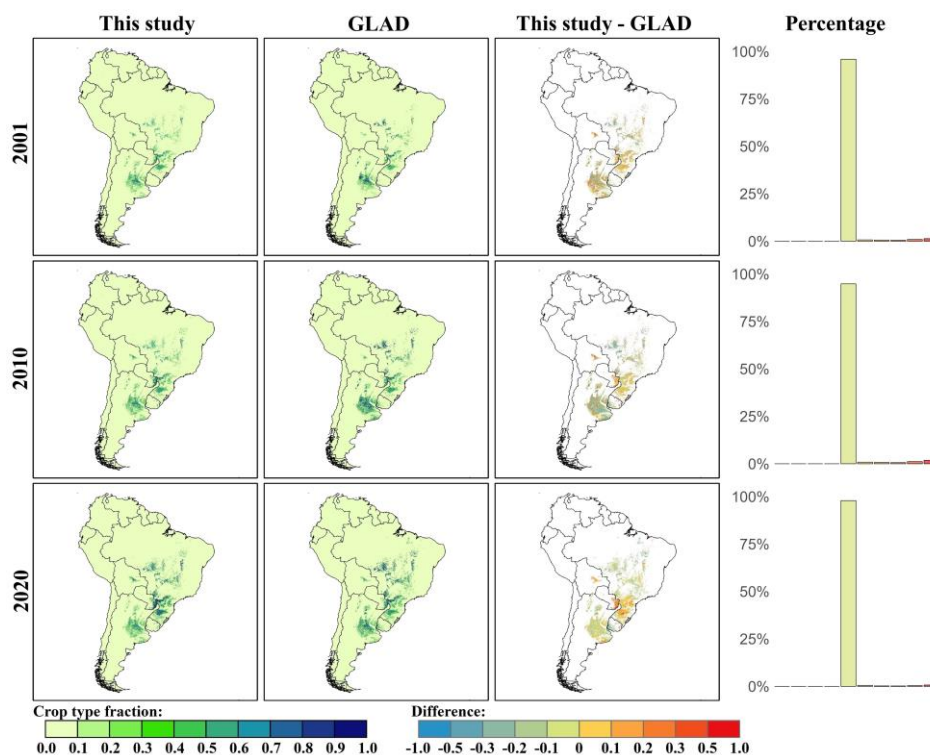


**Figure 10.** Spatial comparison of soybean maps between satellite-based high-resolution data (i.e. GLAD soybean) and the reconstructed data from this study for the years 2001, 2010, and 2020.

## 4 Discussion

### 4.1 Comparison with other datasets

We first compared the area changes of four main crops (maize, rice, soybean, and wheat) in South America from 1950 to 2020 using FAO, GEOGLAM, GLAD, SPAM, and our reconstructed data (Table 4). Before 2000, the soybean area reconstructed in this study was highly consistent with FAO data, but after 2000, the reconstructed soybean area was lower.



This discrepancy mainly originates from countries with larger soybean areas, such as Argentina and Brazil (Figure A6). The census data we used were collected from the national statistical offices and the agricultural census inventory. In contrast, FAO data are mainly provided by  
525 member countries, making it challenging to ensure data accuracy (FAOSTAT). Additionally, Song et al. (2021) reported that the soybean area in the major biomes of South America increased from 26.4 Mha in 2001 to 55.1 Mha in 2019, which is comparable to the data reconstructed in this study and shows greater consistency at the country level. It is worth noting that SPAM also used provincial-level data for modeling, but the total soybean area is consistent  
530 with FAO and higher than that in this study. This is because SPAM corrected the allocation results using FAO national-level data, whereas our results were corrected based on provincial-level statistics (Yu et al., 2020). On the other hand, the soybean area in GEOGLAM is much higher than in other datasets. This difference arises because GEOGLAM integrates crop-specific maps at global and regional scales, spanning a wide range of periods (Becker-Reshef  
535 et al., 2023). For the remaining three crops (i.e., Maize, Wheat, and Rice), our reconstructed data and other datasets showed high agreement across South America. However, the area of maize derived from GEOGLAM data is much higher than the others, for the reasons discussed above. Therefore, due to the lack of high-resolution data for wheat and relatively stable wheat area after 2010, we used only the GEOGLAM wheat distribution map as a base map. Overall,



540 our reconstructed data are in good agreement with other existing datasets and utilize finer-grained statistics to generate spatially explicit crop type distribution maps.

**Table 4.** Comparison of crop-specific areas with other datasets in South America from 1950 to 2020 (Unit: Mha).

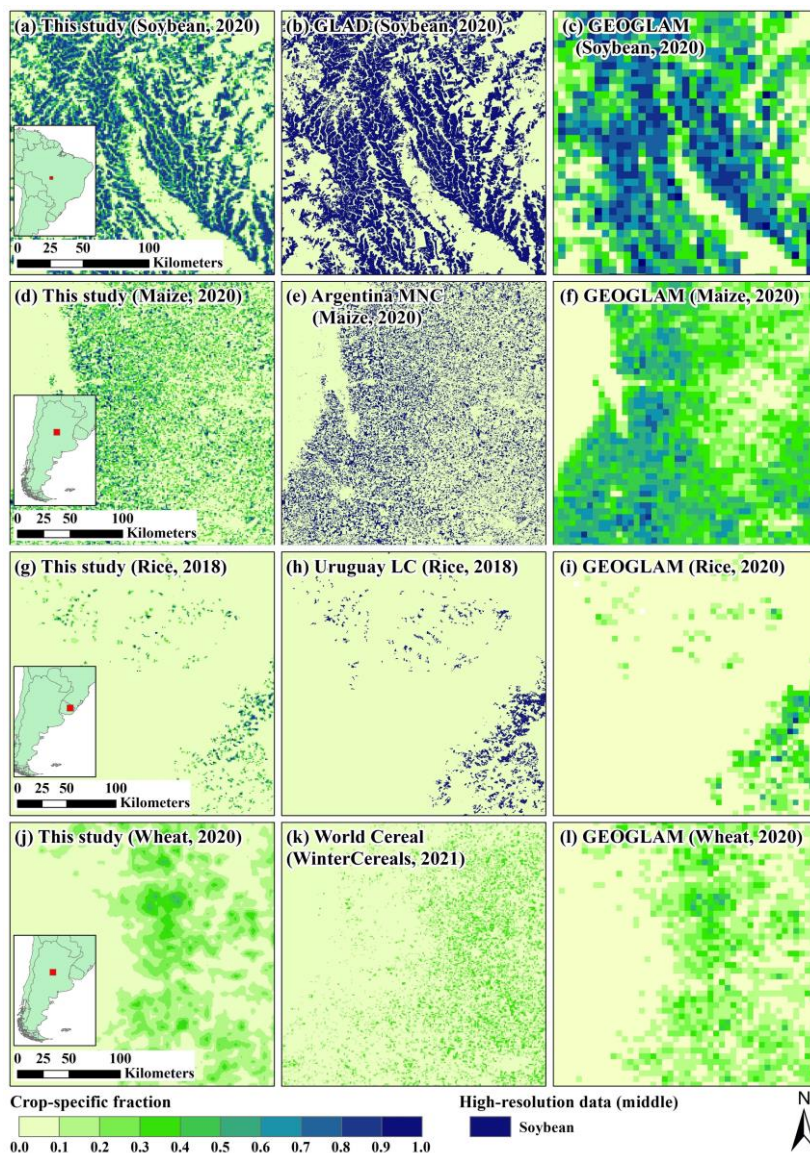
Corps	Year	This study	FAO	SPAM	GEOGLAM
Soybean	1950	0.08	/	/	/
	1980	11.28	11.46	/	/
	2000	25.02	24.17	24.50	/
	2020	48.83	59.89	/	54.05
Maize	1950	12.72	/	/	/
	1980	15.38	16.26	/	/
	2000	16.51	17.70	17.32	/
	2020	26.91	29.23	/	55.45
Wheat	1950	7.62	/	8.90	/
	1980	7.81	9.31	/	/
	2000	7.97	8.32	9.01	/
	2020	7.98	10.41	/	8.83
Rice	1950	3.22	/	/	/
	1980	6.74	7.53	/	/
	2000	4.44	5.66	5.60	/
	2020	3.81	4.13	/	3.52

545 Additionally, we performed a comparison of the distribution of different crop types at both spatial and temporal scales (Figure 11 & 12). Since the lack of other available high-resolution data for maize, wheat, and rice, we first visualized a comparison with the base map (Figure 11). Specifically, the spatial distribution of soybean, maize, and rice is highly consistent with the high-resolution crop-specific distribution maps derived from remote sensing imagery and has



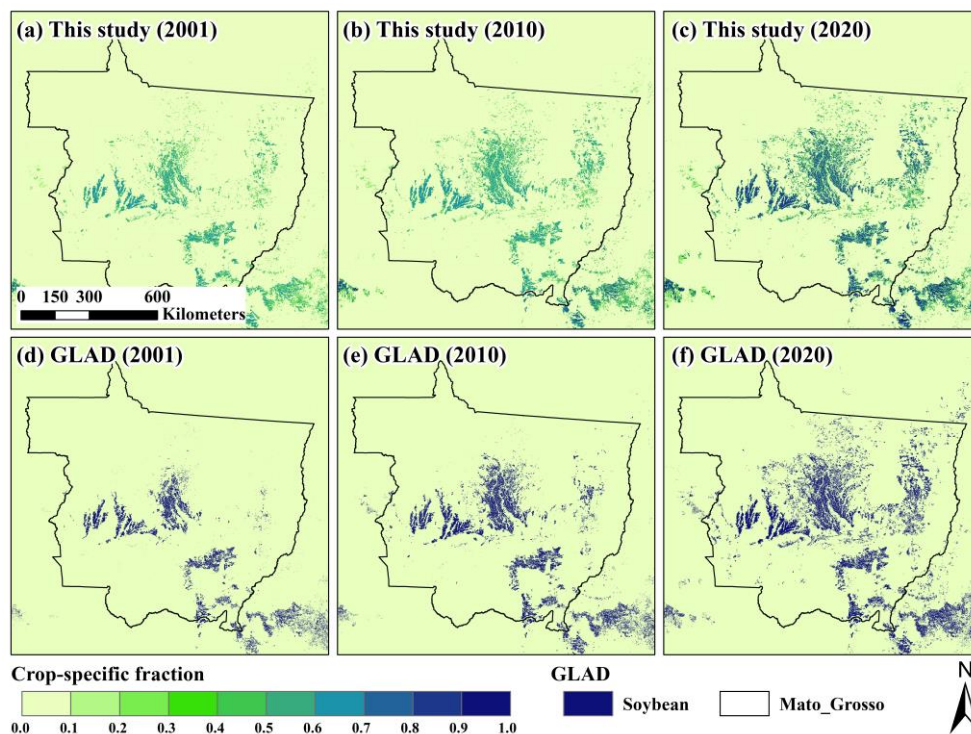
a higher spatial resolution compared to GEOGLAM, providing more detailed information on  
550 crop-specific cultivation patterns. Due to the lack of high-resolution wheat distribution maps,  
we used WorldCereal as a potential wheat distribution map for comparison. The WorldCereal  
is a winter cereal map that includes wheat, barley, and rye (Van Tricht et al., 2023). GLAD,  
being the only soybean distribution maps in South America with a high-resolution and long-  
time series and validation accuracy, allows us to compare spatial distributions of reconstructed  
555 data over time (Song et al., 2021). As shown in Figure 12, we selected the Brazilian state of  
Mato Grosso, one of the most significant regions for soybean expansion since 2000, as an  
example to present comparative results. Comparison results show a relatively high temporal  
agreement between our newly developed data and the GLAD data, demonstrating the reliability  
and accuracy of our data.





560

**Figure 11.** Visual comparison of crop-specific maps between this study and other datasets. The left column shows the crop-specific maps in this study, with high-resolution data in the middle and coarse-resolution data on the right.



565

**Figure 12.** Temporal visual comparison of soybean fraction with GLAD.

## 4.2 Drivers of crop type changes

Agricultural expansion has led to dramatic land use changes in South America over the past few decades (Potapov et al., 2022; Winkler et al., 2021). In this study, we reconstructed the crop-specific maps for South America over the past 70 years by integrating agricultural census data, model-based data, and remote sensing-based crop type data and quantified the land use transitions caused by agricultural expansion. Our results show that the soybean area in South America increased from nearly zero in 1950 to 48.8 Mha in 2020. In South America, soybeans were initially cultivated on small farms primarily to provide animal feed and serve as



a rotation crop adjunct to wheat (Klein and Luna, 2021). By the 1970s, the soybean industry  
575 began to emerge, driven by the surge in global protein meal prices (Richards et al., 2012;  
Warnken, 1999), new geopolitical alliances, and grain-livestock-fuel dynamics (de LT Oliveira,  
2017). Simultaneously, the Brazilian National Agricultural Research Centre of Brazil (i.e.,  
Embrapa) developed new soybean varieties adapted to the tropical climate and successfully  
introduced them to the Cerrado region in the Brazilian Midwest, which contributed to the  
580 “tropicalization of the soybean” and significantly expanded the soybean cultivation area (Klein  
and Luna, 2021). Driven by market-oriented reforms, globalization, and advancements in  
technology, the total soybean exports have burgeoned, further leading to a surge in soybean  
acreage (Song et al., 2021). However, such a dramatic expansion in the soybean area is bound  
to have far-reaching consequences for land use change in South America. Over the past 70  
585 years, soybean expansion has led to the loss of nearly 23.92 Mha of other vegetation, with  
forest accounting for 12.26 Mha, pasture/rangeland for 5.26 Mha, and unmanaged  
grass/shrubland for 6.39 Mha (Table 3). This extensive land use change has led to several  
environmental problems, including biodiversity loss, carbon emissions, land degradation, and  
water pollution (Song et al., 2021; Baumann et al., 2017; Fehlenberg et al., 2017; Pengue, 2005;  
590 Fearnside, 2002). Additionally, maize expansion is also one of the primary factors contributing  
to land use change and environmental threats in South America. Until the 1990s, changes in  
maize area were relatively stable and concentrated in traditional agricultural regions (e.g., the



Pampas region in Argentina and the southern region in Brazil), primarily for domestic consumption as a major source of food for humans and livestock (Warnken, 1999). After the  
595 year 2000, maize cultivation in South America witnessed rapid growth, with maize being widely used not only as a food crop but also for biofuel production (Costantini and Bacenetti, 2021). During this period, maize acreage and yield increased significantly, with Brazil and Argentina becoming two of the world's leading producers and exporters of maize (Klein and Luna, 2022). By 2020, the maize area in South America had increased by a factor of 2.1  
600 compared to 1950, encroaching on a total of 18.35 Mha of other vegetation, including 9.22 Mha of forests, 5.44 Mha of pasture/rangeland, and 3.57 Mha of unmanaged grass/shrubland (Table 3). Despite the importance of soybean and maize in the agricultural expansion of South America, wheat and rice have maintained their position as the main food crops. The expansion of soybean and maize cultivation has largely encroached on non-traditional farmland, such as  
605 forest and pasture, while wheat and rice growing areas have changed less. For wheat and rice, the change in area has remained relatively stable over the past 70 years, generally staying between 5 and 10 Mha (Figure 11). Wheat and rice are grown in relatively stable areas to ensure food security, even though other crops may offer higher economic returns (Jat et al., 2016). Additionally, several governments in South America have traditionally provided sustained  
610 policy support for wheat and rice cultivation, encouraging farmers to maintain a certain level of cultivation to ensure a stable food supply (Warnken, 1999; Altieri, 1992). The more recent



notable expansions in South America invite attention to the broader economic and legal changes that have facilitated or incentivized these drastic farming and agriculture changes, including through capital, finance, trade and investment dynamics (Pistor, 2019; Saab, 2018).

### 615 **4.3 Uncertainties**

This study provides a set of crop type data with  $1 \text{ km} \times 1 \text{ km}$  resolution and annual steps from 1950 to 2020 in South America. The evaluation at different scales (i.e., provincial, municipal, and grid levels) showed that our reconstructed data are comparable to other datasets. However, some limitations and uncertainties remain in this study. (1) The base maps of  
620 cropland density and crop types are crucial for constraining the spatial patterns of crops. In general, reconstructing historical crop type distributions requires using the present crop type distribution as a benchmark to project back into the past (Adalibieke et al., 2023; Ye et al., 2023). In this study, we used several high-resolution remote sensing products (i.e., Argentina MNC, MapBiomass, and Uruguay LC) to construct a base map. However, it does not cover the  
625 entire South America and exhibits some temporal variability. Therefore, we used SPAM2010 as a supplement for areas where high-resolution data were not available and eventually corrected all base maps using inventory data in 2020. This approach may overlook certain spatial details in some regions. (2) In some countries, historical agricultural census data are limited at the provincial level. Adequate historical agricultural census data is the basis for the



630 reconstruction of historical spatial data. Although provincial-level data are available in every  
country, only a few years of data are accessible in some countries due to inconsistencies in  
national policies and agricultural census years. Even though this data can be reconstructed in  
various ways (i.e., interpolation) (Li et al., 2023; Mao et al., 2023), some uncertainties remain.  
Finally, national-level trends and interpolation methods were used to reconstruct provincial-  
635 level data, which to some extent may miss internal trends of some provinces. Interannual  
variability at the provincial level is generally not fully consistent with that at the national level,  
and such reconstruction methods may introduce some overestimation or underestimation of the  
results. (3) Due to the lack of high-resolution crop type maps and reliable historical statistics,  
only four crops (i.e., soybean, maize, wheat, and rice) were included in this study. (4) Due to  
640 the lack of accurate crop distribution information, crop rotation was not considered in this study.  
Ye et al. (2024) considered crop rotation to reconstruct the historical crop distribution maps for  
the United States, relying on Cropland Data Layer (CDL) data for crop rotation information;  
however, similar high-resolution products are lacking for South America. Although Pott et al.  
(2023) visualized crop rotation information for soybean, maize, and rice in Rio Grande do Sul,  
645 southern Brazil, it did not sufficiently represent the overall rotation patterns across South  
America. Therefore, future research should focus on crop type mapping in South America to  
obtain crop rotation patterns, enabling the generation of more accurate historical crop-specific  
maps in subsequent HISLAND-SA versions. Despite these limitations and uncertainties, this



study is still the first attempt at crop type reconstruction in South America and has significant  
650 implications for analysing the impacts of agricultural expansion on local livelihoods and food  
security, trade and agricultural support policies.

## 5 Data and code availability

The developed dataset and codes are available at <https://doi.org/10.5281/zenodo.14002960> (Xu  
et al., 2024). The annual and 1-km crop-specific gridded data with GeoTiff format. The state  
655 mask with shapefile and GeoTiff formats are also provided.

## 6 Conclusions

In this study, we developed spatially explicit crop-specific maps (i.e., soybean, maize,  
wheat, and rice) at a 1 km  $\times$  1 km resolution and annual step in South America from 1950 to  
2020 by integrating historical agricultural census data, model-based crop type data, and high-  
660 resolution remote sensing-based crop type data. The results showed that agricultural expansion  
has severely encroached on the other vegetation of South America over the past 70 years.  
Specifically, soybean is one of the most dramatically expanded crops increasing from  
essentially zero in 1950 to 48.8 Mha in 2020, resulting in a total loss of 23.92 Mha of other  
vegetation. Additionally, the maize area in South America had increased from 12.7 Mha in  
665 1950 to 26.9 Mha in 2020, encroaching on a total of 18.35 Mha of other vegetation. In contrast,



the area of wheat and rice kept relatively stable. Compared with existing data, our reconstructed data have higher spatial and temporal resolution which can better capture the dynamics of crop type changes during the historical period. Overall, this newly developed data can be used to assess the impacts of agricultural expansion on greenhouse gas emissions, ecosystem services, biodiversity loss, and to guide the formulation of land management and conservation policies for sustainable agricultural development and ecological conservation.

## Appendix A

**Table A1.** The number of provinces in each country of South America.

Country	GADM Provinces	Units in this study	Available census data
Argentina	24	23	5
Bolivia	9	9	40
Brazil	27	27	8
Chile	16	16	2
Colombia	33	32	7
French Guiana	2	1	/
Ecuador	24	24	3
Guyana	10	10	11
Paraguay	18	17	21
Peru	26	24	1
Suriname	10	10	2
Uruguay	19	19	2
Venezuela	25	25	1
<b>Total</b>	<b>243</b>	<b>237</b>	<b>103</b>





675 **Table A2.** Definitions of different cropland datasets.

<b>Datasets</b>	<b>Definition</b>
HYDE	After 1960 identical to FAO's category: Arable land and permanent crops.
ESA CCI	(1) 10: Cropland, rainfed (2) 20: Cropland, irrigated or post-flooding (3) 30: Mosaic cropland (> 50%) / natural vegetation (tree, shrub, herbaceous cover) (< 50%)
GLAD GCC	(1) Annual and perennial herbaceous crops for human consumption, forage (including hay), and biofuel. (2) Perennial woody crops, permanent pastures, and shifting cultivation are excluded from the definition.
GLC FCS30D	(1) 10: Rained cropland (2) 11: Herbaceous cover cropland (3) 12: Tree or shrub (Orchard) cropland (4) 20: Irrigated cropland
CGLS-LC100	Cultivated and managed vegetation/agriculture: Lands covered with temporary crops followed by harvest and a bare soil period (e.g., single, and multiple cropping systems). Note that perennial woody crops will be classified as the appropriated forest or shrub land cover type.

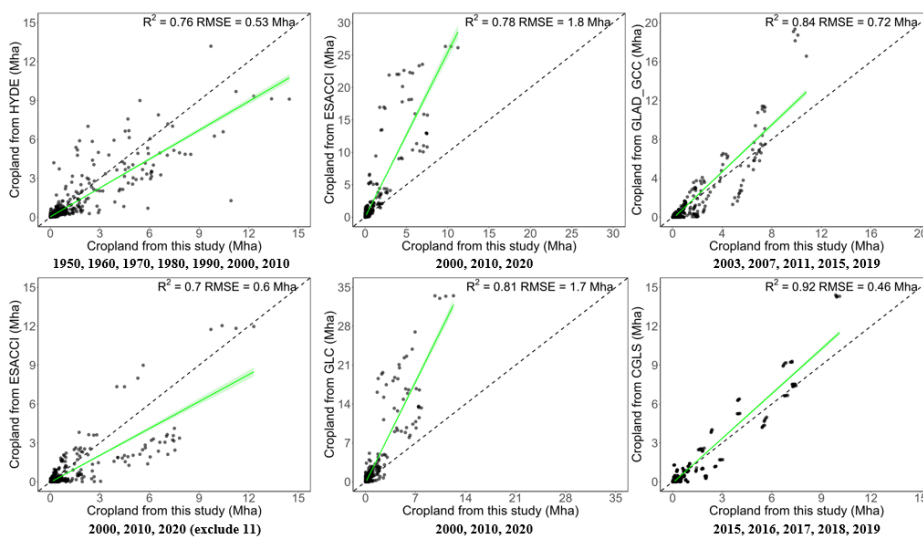
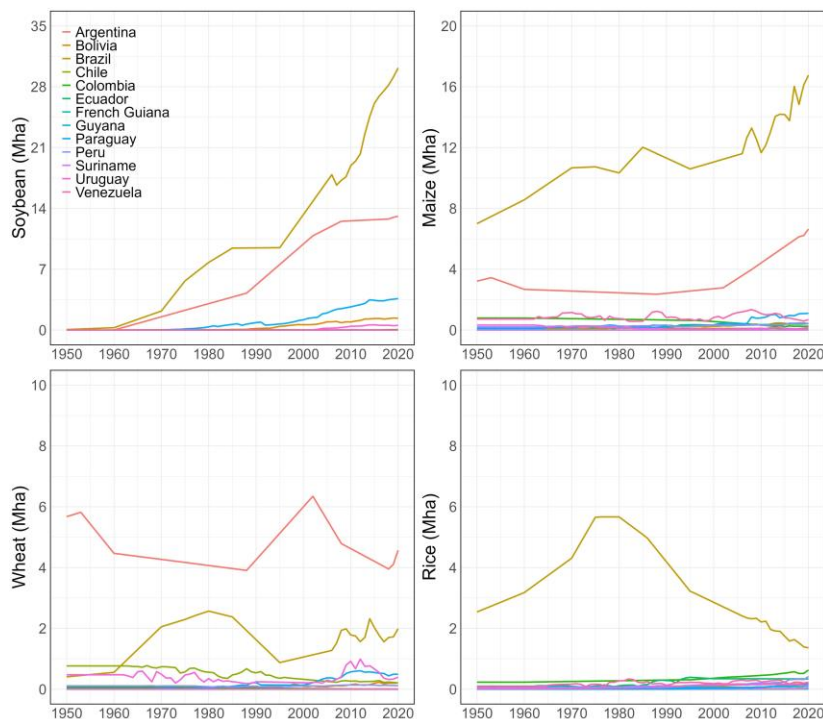


**Figure A1.** Comparisons between reconstructed cropland area and other datasets at the provincial level.



680 **Figure A2.** Temporal changes in crop-specific areas in South America at the country level during 1950-2020.

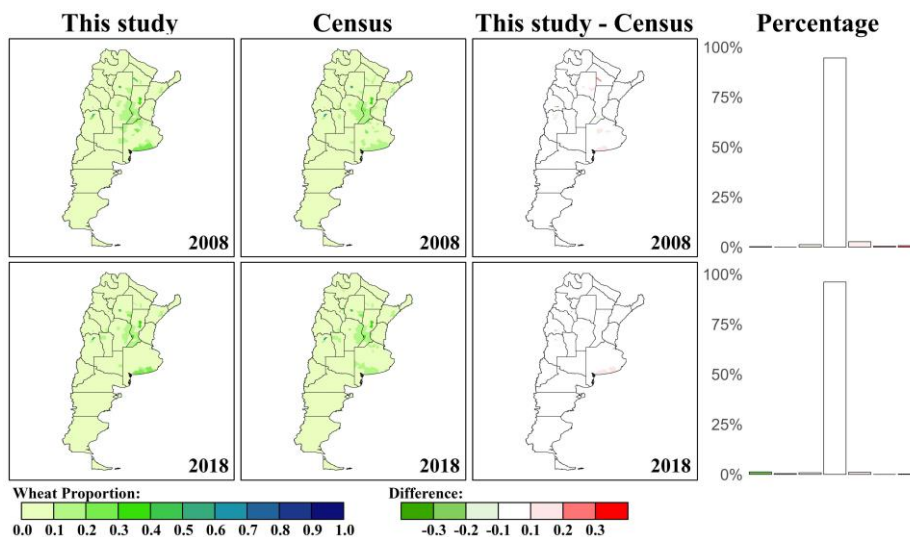


**Figure A3.** Spatial comparison of the wheat proportion (i.e., rice area/municipal area) between this study and census data at the municipal level in Argentina (2008 and 2018). Left column: wheat proportion from this study; Middle column: wheat proportion from census data; Right column: the difference in wheat proportion between this study and census data.

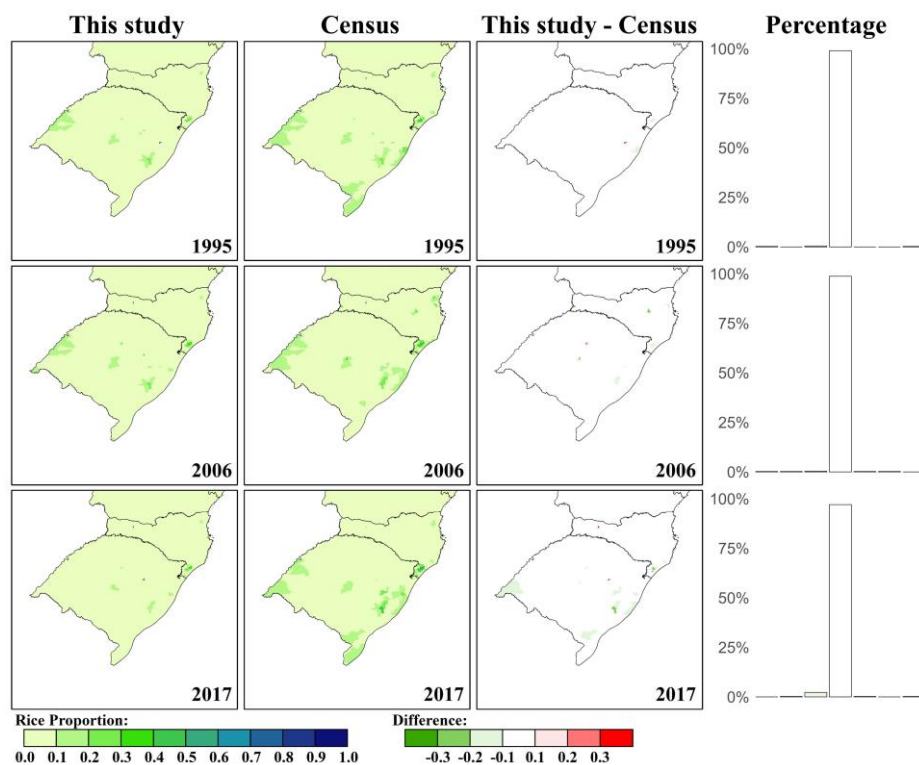


**Figure A4.** Spatial comparison of the rice proportion (i.e., rice area/municipal area) between this study and census data at the municipal level in Rio Grande do Sul in Brazil (1995, 2006, and 2017). Left column: rice proportion  
690 from this study; Middle column: rice proportion from census data; Right column: the difference in rice proportion  
between this study and census data.

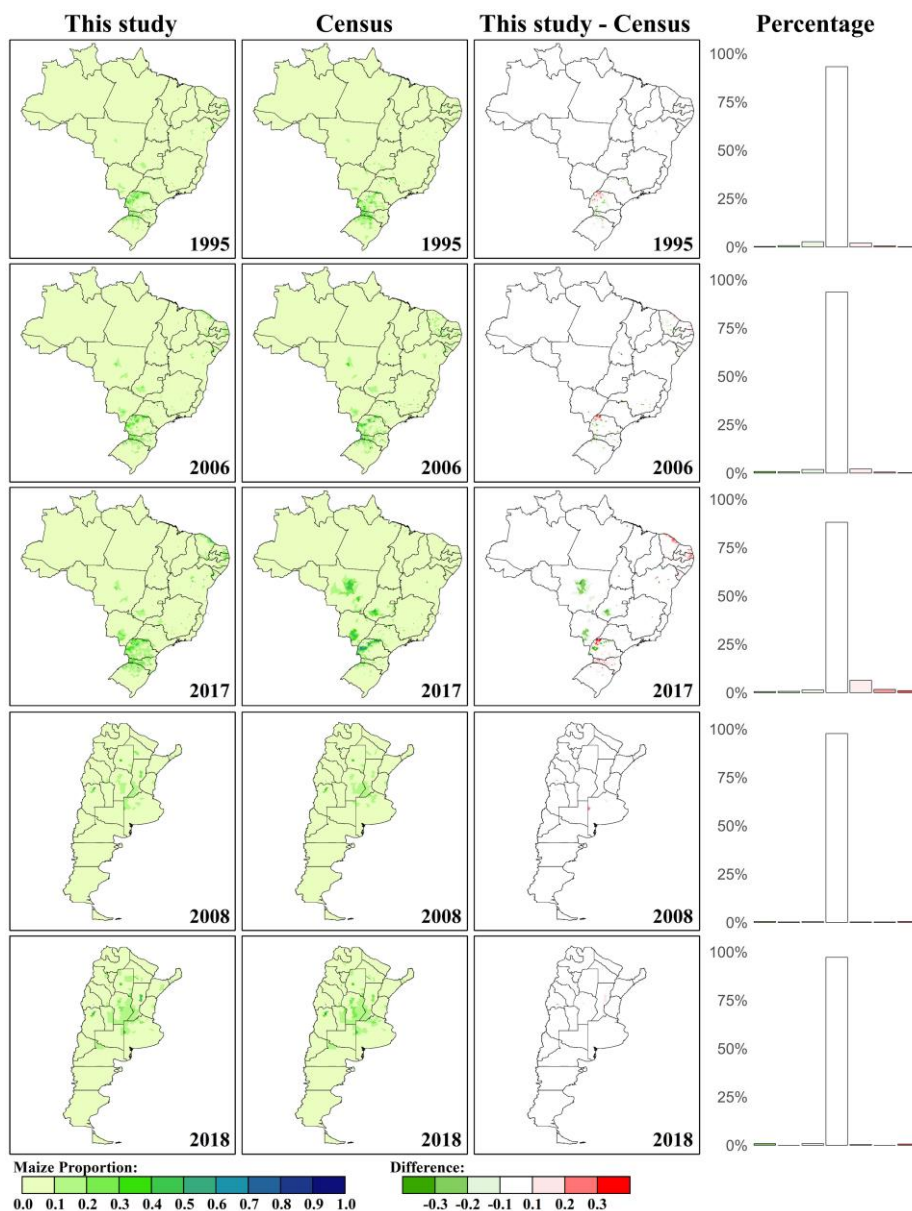
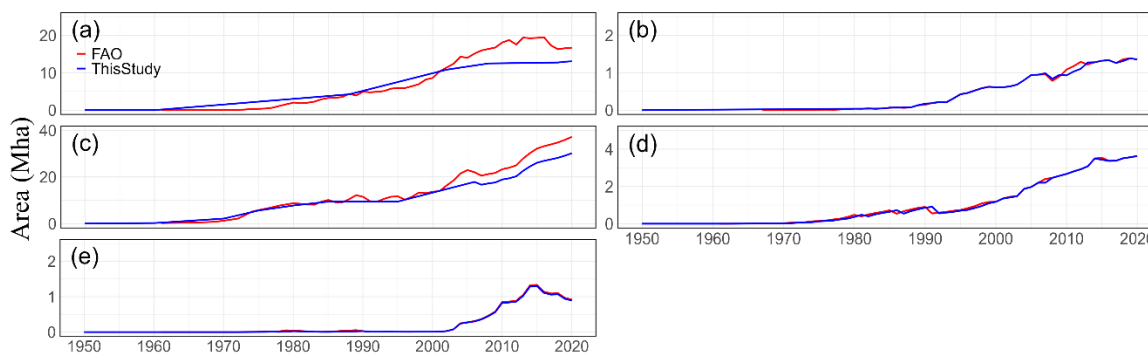


**Figure A5.** Spatial comparison of the maize proportion (i.e., maize area/municipal area) between this study and census data at the municipal level in Argentina (2008 and 2018) and Brazil (1995, 2006, and 2017). Left column: 695 maize proportion from this study; Middle column: maize proportion from census data; Right column: the difference in maize proportion between this study and census data.



700 **Figure A6.** Comparison of soybean areas with FAO data in South America at the country level. (a) Argentina, (b) Bolivia, (c) Brazil, (d) Paraguay, (e) Uruguay.

### Competing interests

At least one of the (co-)authors is a member of the editorial board of Earth System Science Data.

### Acknowledgements

705 We thank the national statistical bureaus in Argentina, Bolivia, Brazil, Chile, Colombia, Ecuador, Guyana, Paraguay, Peru, Suriname, Uruguay and Venezuela for providing essential agricultural census data that supported this research.

### Financial support

This study has been supported by the Centre for Earth System Science and Global  
710 Sustainability and Global Carbon Project (GCP) Boston Office at Boston College.



## References

- OAS. (2024). Organization of American States: Special Rapporteurship on Economic, Social, Cultural and Environmental Rights, A hemispheric agenda for ESCER: Work plan 2024-2026, Javier Palummo Lantes.
- Xu, B., H. Tian, S. Pan, X. Li, R. Meng, Ó. Melo, M. d. I. Á. Picone, X.-P. Song, E. Severnini, K. G. Young, and F. & Zhao (2024), HISLAND-SA: Annual and 1-km crop-specific gridded data in South America from 1950 to 2020, edited, Zenodo, doi:<https://doi.org/10.5281/zenodo.14002960>.
- 715
- Ye, S., P. Cao, and C. Lu. (2024). Annual time-series 1 km maps of crop area and types in the conterminous US (CropAT-US): cropping diversity changes during 1850–2021. *Earth System Science Data*, 16(7), 3453-3470. <https://doi.org/10.5194/essd-16-3453-2024>.
- 720
- Zhang, X., T. Zhao, H. Xu, W. Liu, J. Wang, X. Chen, and L. Liu. (2024). GLC\_FCS30D: the first global 30 m land-cover dynamics monitoring product with a fine classification system for the period from 1985 to 2022 generated using dense-time-series Landsat imagery and the continuous change-detection method. *Earth System Science Data*, 16(3), 1353-1381. <https://10.5194/essd-16-1353-2024>.
- Adalibieke, W., X. Cui, H. Cai, L. You, and F. Zhou. (2023). Global crop-specific nitrogen fertilization dataset in 1961-2020. *Sci Data*, 10(1), 617. <https://10.1038/s41597-023-02526-z>.
- 725
- Becker-Reshef, I., B. Barker, A. Whitcraft, P. Oliva, K. Mobley, C. Justice, and R. Sahajpal. (2023). Crop Type Maps for Operational Global Agricultural Monitoring. *Sci Data*, 10(1), 172. <https://10.1038/s41597-023-02047-9>.
- Boyd, W. (2023), Food law's agrarian question: capital, global farmland, and food security in an age of climate disruption, in *Research Handbook on International Food Law*, edited, pp. 29-62, Edward Elgar Publishing.
- 730
- Cheng, N. F. L., A. S. Hasanov, W. C. Poon, and E. Bouri. (2023). The US-China trade war and the volatility linkages between energy and agricultural commodities. *Energy Economics*, 120. <https://10.1016/j.eneco.2023.106605>.
- Li, X., H. Tian, C. Lu, and S. Pan. (2023). Four-century history of land transformation by humans in the United States (1630–2020): annual and 1 km grid data for the HISTORY of LAND changes (HISLAND-US). *Earth System Science Data*, 15(2), 1005-1035. <https://10.5194/essd-15-1005-2023>.
- 735
- Mao, F., X. Li, G. Zhou, Z. Huang, Y. Xu, Q. Chen, M. Yan, J. Sun, C. Xu, and H. Du. (2023). Land use and cover in subtropical East Asia and Southeast Asia from 1700 to 2018. *Global and Planetary Change*, 226. <https://10.1016/j.gloplacha.2023.104157>.
- 740
- Pott, L. P., T. J. C. Amado, R. A. Schwalbert, G. M. Corassa, and I. A. Ciampitti. (2023). Mapping crop rotation by satellite-based data fusion in Southern Brazil. *Computers and Electronics in Agriculture*, 211. <https://10.1016/j.compag.2023.107958>.



- 745 Tang, F. H. M., T. H. Nguyen, G. Conchedda, L. Casse, F. N. Tubiello, and F. Maggi. (2023). CROPGRIDS: A global geo-referenced dataset of 173 crops circa 2020. *Earth Syst. Sci. Data Discuss.*, 2023, 1-22. <https://10.5194/essd-2023-130>.
- 750 Van Tricht, K., J. Degerickx, S. Gilliams, D. Zanaga, M. Battude, A. Grosu, J. Brombacher, M. Lesiv, J. C. L. Bayas, S. Karanam, S. Fritz, I. Becker-Reshef, B. Franch, B. Mollà-Bononad, H. Boogaard, A. K. Pratihast, B. Koetz, and Z. Szantoi. (2023). WorldCereal: a dynamic open-source system for global-scale, seasonal, and reproducible crop and irrigation mapping. *Earth System Science Data*, 15(12), 5491-5515. <https://10.5194/essd-15-5491-2023>.
- Ye, S., P. Cao, and C. Lu. (2023). Annual time-series 1-km maps of crop area and types in the conterminous US (CropAT-US): cropping diversity changes during 1850–2021. *Earth System Science Data*, 2023, 1-24.
- 755 Erenstein, O., M. Jaleta, K. A. Mottaleb, K. Sonder, J. Donovan, and H.-J. Braun (2022), Global trends in wheat production, consumption and trade, in *Wheat improvement: food security in a changing climate*, edited, pp. 47-66, Springer International Publishing Cham.
- IPCC (2022), Impacts, adaptation and vulnerability. Summary for policymakers *Rep.*, 37 pp.
- Klein, H. S., and F. V. Luna. (2022). The impact of the rise of modern maize production in Brazil and Argentina. *Historia agraria: Revista de agricultura e historia rural*(86), 273-310.
- 760 Potapov, P., S. Turubanova, M. C. Hansen, A. Tyukavina, V. Zalles, A. Khan, X. P. Song, A. Pickens, Q. Shen, and J. Cortez. (2022). Global maps of cropland extent and change show accelerated cropland expansion in the twenty-first century. *Nat Food*, 3(1), 19-28. <https://10.1038/s43016-021-00429-z>.
- Clapp, J. (2021). The problem with growing corporate concentration and power in the global food system. *Nature Food*, 2(6), 404-408. <https://doi.org/10.1038/s43016-021-00297-7>.
- 765 Costantini, M., and J. Bacenetti. (2021). Soybean and maize cultivation in South America: Environmental comparison of different cropping systems. *Cleaner Environmental Systems*, 2. <https://10.1016/j.cesys.2021.100017>.
- Klein, H. S., and F. V. Luna. (2021). The growth of the soybean frontier in South America: The case of Brazil and Argentina. *Revista de Historia Economica-Journal of Iberian and Latin American Economic History*, 39(3), 427-468. <https://10.1017/S0212610920000269>.
- 770 Song, X. P., M. C. Hansen, P. Potapov, B. Adusei, J. Pickering, M. Adami, A. Lima, V. Zalles, S. V. Stehman, C. M. Di Bella, M. C. Conde, E. J. Copati, L. B. Fernandes, A. Hernandez-Serna, S. M. Jantz, A. H. Pickens, S. Turubanova, and A. Tyukavina. (2021). Massive soybean expansion in South America since 2000 and implications for conservation. *Nat Sustain*, 2021. <https://doi.org/10.1038/s41586-018-0411-9>.
- 775 Winkler, K., R. Fuchs, M. Rounsevell, and M. Herold. (2021). Global land use changes are four times greater than previously estimated. *Nature Communications*, 12(1). <https://10.1038/s41467-021-22702-2>.





- Zalles, V., M. C. Hansen, P. V. Potapov, D. Parker, S. V. Stehman, A. H. Pickens, L. L. Parente, L. G. Ferreira, X.-P. Song, and A. Hernandez-Serna. (2021). Rapid expansion of human impact on natural land in South America since 1985. *Science Advances*, 7(14), eabg1620. <https://10.1126/sciadv.abg1620>.
- 780 Buchhorn, M., M. Lesiv, N.-E. Tsendbazar, M. Herold, L. Bertels, and B. Smets. (2020). Copernicus Global Land Cover Layers—Collection 2. *Remote Sensing*, 12(6). <https://10.3390/rs12061044>.
- De Abelleira, D., S. R. Veron, S. Banchemo, M. J. Mosciaro, A. Franzoni, M. A. Boasso, S. O. Valiente, O. Puig, S. Y. Goytia, and M. D. R. M. Iturralde Elortegui (2020), Mapa Nacional De Cultivos. Campaña 2019/2020. Versión 1 Publicación No. 2Rep., INTA, <https://hdl.handle.net/20.500.12123/8113>.
- 785 FAO (2020), Food and Agriculture Organization of the United Nations, edited, FAOSTAT Statistical Database. Retrieved from <http://www.fao.org/faostat/en/>.
- Yu, Q., L. You, U. Wood-Sichra, Y. Ru, A. K. B. Joglekar, S. Fritz, W. Xiong, M. Lu, W. Wu, and P. Yang. (2020). A cultivated planet in 2010 – Part 2: The global gridded agricultural-production maps. *Earth System Science Data*, 12(4), 3545-3572. <https://10.5194/essd-12-3545-2020>.
- 790 Petraglia, C., M. Dell'Acqua, G. Pereira, and E. Yussim. (2019). Mapa integrado de cobertura/uso del suelo del Uruguay, año 2018. *Anuario OPYPA*, 27.
- Pistor, K. (2019). The code of capital: How the law creates wealth and inequality.
- Renard, D., and D. Tilman. (2019). National food production stabilized by crop diversity. *Nature*, 571(7764), 257-260. <https://doi.org/10.1038/s41586-019-1316-y>.
- 795 Tsendbazar, N., M. Herold, M. Lesiv, and S. Fritz. (2019). Copernicus Global Land Service: Land Cover 100m: Version 2 Globe 2015: Validation Report. *Zenodo: Geneve, Switzerland*. <https://https://doi.org/10.5281/zenodo.3243509>.
- Saab, A. (2018). An international law approach to food regime theory. *Leiden Journal of International Law*, 31(2), 251-265. <https://10.1017/S0922156518000122>.
- 800 Song, X.-P., M. C. Hansen, S. V. Stehman, P. V. Potapov, A. Tyukavina, E. F. Vermote, and J. R. Townshend. (2018). Global land change from 1982 to 2016. *Nature*, 560(7720), 639-643. <https://doi.org/10.1038/s41586-018-0411-9>.
- Baumann, M., I. Gasparri, M. Piquer-Rodriguez, G. Gavier Pizarro, P. Griffiths, P. Hostert, and T. Kuemmerle. (2017). Carbon emissions from agricultural expansion and intensification in the Chaco. *Glob Chang Biol*, 23(5), 1902-1916. <https://10.1111/gcb.13521>.
- 805 de LT Oliveira, G. (2017), The geopolitics of Brazilian soybeans, in *Soy, Globalization, and Environmental Politics in South America*, edited, pp. 98-122, Routledge, <https://10.1080/03066150.2014.992337>.



- Fehlenberg, V., M. Baumann, N. I. Gasparri, M. Piquer-Rodriguez, G. Gavier-Pizarro, and T. Kuemmerle. (2017). The role of soybean production as an underlying driver of deforestation in the South American Chaco. *Global Environmental Change*, 45, 24-34. <https://10.1016/j.gloenvcha.2017.05.001>.
- 810 He, C., Z. Liu, M. Xu, Q. Ma, and Y. Dou. (2017). Urban expansion brought stress to food security in China: Evidence from decreased cropland net primary productivity. *Sci Total Environ*, 576, 660-670. <https://10.1016/j.scitotenv.2016.10.107>.
- Klein Goldewijk, K., A. Beusen, J. Doelman, and E. Stehfest. (2017). Anthropogenic land use estimates for the Holocene – HYDE 3.2. *Earth System Science Data*, 9(2), 927-953. <https://10.5194/essd-9-927-2017>.
- 815 Souza, C., and T. Azevedo. (2017). MapBiomas general handbook. *MapBiomas: São Paulo, Brazil*, 1-23. <https://10.13140/RG.2.2.31958.88644>.
- Yu, Z., and C. Lu. (2017). Historical cropland expansion and abandonment in the continental U.S. during 1850 to 2016. *Global Ecology and Biogeography*, 27(3), 322-333. <https://10.1111/geb.12697>.
- 820 Jat, M. L., J. C. Dagar, T. B. Sapkota, B. Govaerts, S. Ridaura, Y. S. Saharawat, R. K. Sharma, J. Tatarwal, R. K. Jat, and H. Hobbs. (2016). Climate change and agriculture: adaptation strategies and mitigation opportunities for food security in South Asia and Latin America. *Advances in agronomy*, 137, 127-235. <https://doi.org/10.1016/bs.agron.2015.12.005>.
- 825 Ceddia, M. G., N. O. Bardsley, S. Gomez-y-Paloma, and S. Sedlacek. (2014). Governance, agricultural intensification, and land sparing in tropical South America. *Proc Natl Acad Sci U S A*, 111(20), 7242-7247. <https://10.1073/pnas.1317967111>.
- Meyfroidt, P., K. M. Carlson, M. E. Fagan, V. H. Gutiérrez-Vélez, M. N. Macedo, L. M. Curran, R. S. DeFries, G. A. Dyer, H. K. Gibbs, and E. F. Lambin. (2014). Multiple pathways of commodity crop expansion in tropical forest landscapes. *Environmental Research Letters*, 9(7), 074012. <https://10.1088/1748-9326/9/7/074012>.
- 830 Tian, H., K. Banger, T. Bo, and V. K. Dadhwal. (2014). History of land use in India during 1880–2010: Large-scale land transformations reconstructed from satellite data and historical archives. *Global and Planetary Change*, 121, 78-88. <https://10.1016/j.gloplacha.2014.07.005>.
- Campos Matos, C. C. (2013). Economic impact of agriculture trade liberalization in Argentina (Doctoral dissertation, KDI School).
- 835 Garrett, R. D., X. Rueda, and E. F. Lambin. (2013). Globalization’s unexpected impact on soybean production in South America: linkages between preferences for non-genetically modified crops, eco-certifications, and land use. *Environmental Research Letters*, 8(4), 044055. <https://10.1088/1748-9326/8/4/044055>.
- Richards, P. D., R. J. Myers, S. M. Swinton, and R. T. Walker. (2012). Exchange rates, soybean supply response, and deforestation in South America. *Global Environmental Change*, 22(2), 454-462. <https://10.1016/j.gloenvcha.2012.01.004>.



- 840 Frison, E. A., J. Chérfa, and T. Hodgkin. (2011). Agricultural biodiversity is essential for a sustainable improvement in food and nutrition security. *Sustainability*, 3(1), 238-253. <https://doi.org/10.3390/su3010238>.
- Dawe, D., S. Block, A. Gulati, J. Huang, and S. Ito (2010), Domestic rice price, trade, and marketing policies, in *Rice in the global economy: strategic research and policy issues for food security*. Los Baños, Philippines, International Rice Research Institute. 477p, edited, [https://books.irri.org/9789712202582\\_content](https://books.irri.org/9789712202582_content).
- 845 Mueller, C., and B. Mueller (2010), The evolution of agriculture and land reform in Brazil, 1960–2006, in *Economic Development in Latin America: Essay in Honor of Werner Baer*, edited, pp. 133-162, Springer, [https://doi.org/10.1057/9780230297388\\_10](https://doi.org/10.1057/9780230297388_10).
- Monfreda, C., N. Ramankutty, and J. A. Foley. (2008). Farming the planet: 2. Geographic distribution of crop areas, yields, physiological types, and net primary production in the year 2000. *Global Biogeochemical Cycles*, 22(1). <https://doi.org/10.1029/2007gb002947>.
- 850 Foley, J. A., R. DeFries, G. P. Asner, C. Barford, G. Bonan, S. R. Carpenter, F. S. Chapin, M. T. Coe, G. C. Daily, and H. K. Gibbs. (2005). Global consequences of land use. *science*, 309(5734), 570-574. <https://doi.org/10.1126/science.1111772>.
- Pengue, W. A. (2005). Transgenic crops in Argentina: the ecological and social debt. *Bulletin of Science, Technology & Society*, 25(4), 314-322. <https://doi.org/10.1177/0270467605277290>.
- 855 Fearnside, P. M. (2002). Soybean cultivation as a threat to the environment in Brazil. *Environmental Conservation*, 28(1), 23-38. <https://doi.org/10.1017/s0376892901000030>.
- Warnken, P. F. (1999). The development and growth of the soybean industry in Brazil. (*No Title*).
- De Janvry, A., E. Sadoulet, and W. Wolford. (1998). The changing role of the state in Latin American land reforms. <https://doi.org/10.1093/acprof:oso/9780199242177.003.0011>.
- 860 Munoz, J., and I. Lavadenz. (1997). Reforming the agrarian reform in Bolivia. <https://doi.org/10.22004/ag.econ.294410>.
- Altieri, M. A. (1992). Sustainable agricultural development in Latin America: exploring the possibilities. *Agriculture, ecosystems & environment*, 39(1-2), 1-21. [https://doi.org/10.1016/0167-8809\(92\)90202-M](https://doi.org/10.1016/0167-8809(92)90202-M).
- Chonchol, J. (1990). Agricultural modernization and peasant strategies in Latin America. *International Social Science Journal*, 42(124). <https://unesdoc.unesco.org/ark:/48223/pf0000088259>.
- 865 FAOSTAT. Production/Crops and livestock products - Metadata.